

CZECH UNIVERSITY OF LIFE SCIENCES
PRAGUE

FACULTY OF ENVIRONMENTAL SCIENCES

Impact assessment of urban development on urban heat
island effect in Prague

DIPLOMA THESIS

Supervisor: doc. Mgr. Jitka Kumhálová, Ph.D.

Author: Bc. Tomáš Sedláček

2018

CZECH UNIVERSITY OF LIFE SCIENCES PRAGUE

Faculty of Environmental Sciences

DIPLOMA THESIS ASSIGNMENT

Bc. Tomáš Sedláček

Landscape Planning

Thesis title

Impact assessment of urban development on urban heat island effect in Prague

Objectives of thesis

Assess how urban development of Prague affected intensity of urban heat island in selected time period. Determine relations of urban heat island and its specific factors. Predict future possible intensity of urban heat island, based on current zoning plan of Prague.

Methodology

- 1) Literal review on the process of urban development and its Prague context, UHI and processing of satellite images.
- 2) Selecting satellite images of Prague based on the most suitable meteorological conditions.
- 3) Pre-processing of satellite images.
- 4) Determine quantitative representation of UHI, extraction of impervious surfaces (NDCI) and density of vegetation (NDVI).
- 5) Analyse relations between UHI, NDCI and NDVI.
- 6) Predict future intensity of UHI based on current zoning plan of Prague.

The proposed extent of the thesis

40-80 pages

Keywords

Urban heat island effect, Remote sensing, GIS, Urban development, NDCI, NDVI

Recommended information sources

- GUNAWARDENA K. R. et al. (2017): Utilising green and bluespace to mitigate urban heat island intensity. University of Bath, Claverton Down, Bath, United Kingdom
- SINGH P. et al. (2016): Impact of land use change and urbanization on urban heat island in Lucknow city, Central India. A remote sensing based estimate. Amity University-Sector 125, Noida, India
- SON N. et al. (2016): Assessment of urbanization and urban heat islands in Ho Chi Minh City, Vietnam using Landsat data. National Central University, Jhongli District, Taoyuan City, Taiwan
- U.S. ENVIRONMENTAL PROTECTION AGENCY. (2012): Reducing urban heat islands: Compendium of strategies. (online) Available at: <https://www.epa.gov/heat-islands/heat-island-compendium> (Accessed 3rd of December 2017)
- ZEMEK F. (2013): Aerial remote sensing. Centrum výzkumu globální změny AV Č. Brno. Czech Republic
-

Expected date of thesis defence

2017/18 SS – FES

The Diploma Thesis Supervisor

doc. Mgr. Jitka Kumhálová, Ph.D.

Supervising department

Department of Machinery Utilization

Electronic approval: 22. 3. 2018

doc. Ing. Petr Šařec, Ph.D.

Head of department

Electronic approval: 26. 3. 2018

prof. RNDr. Vladimír Bejček, CSc.

Dean

Prague on 16. 04. 2018

Declaration

I hereby declare that the work presented in this thesis is, to the best of my knowledge and belief, original, except as cited in the text, and that the material has not been submitted, either in whole or in part, for degree at this or any other university. I have listed all literature and publications from which I have acquired information.

Prague, 16th of April, 2018

Bc. Tomáš Sedláček

Acknowledgement

I would like to thank the supervisor of this thesis doc. Mgr. Jitka Kumhálová, Ph.D. for an guidance with this work and her help with data interpretation. I would like to also thank Ing. David Moravec for his help with data pre-processing and last but not least I would like to thank Tereza Dolášová for her limitless support.

Abstract

This thesis examines the impact of urban development on the *urban heat island* (UHI) between years 2002 and 2016 in Prague by remote sensing approach. The main factors are the *normalized difference vegetation index* (NDVI), the *build-up index* (BI) created by author and statistical data on the numbers of newly arrived people into individual urban zones of Prague. For the quantitative interpretation of the UHI, the *urban thermal field variance index* (UTFVI) was used, which also describes the degree of ecological vulnerability. *Land surface temperature* (LST) has been interpreted in two ways for better comparison with other factors. The first way is the difference between years and the second is the classification of individual years using *Nature Breaks (Jenks)* method. Individual urban zones have experienced different spatial development, so the author used the division into four concentric zones: *downtown, inner city, outer city and outskirt*. The image from 2002 was acquired by Landsat 7 (ETM +) satellite and the second image from 2016 was acquired by Landsat 8 (OLI and TIRS) satellite, both in the 30-metres resolution. For comparison it was necessary to determine the appropriate classification of the differences of the individual years, due to various influences of e.g. different vegetation period, surfaces swaps, etc. For a better accuracy of results, arable land was erased from the final outputs before comparison was made. For the year 2016, extraction of *impervious surfaces* (IS) was carried out using a combination of BI and spatial data from the current Master plan (MP) of Prague. Thanks to the knowledge of the exact spatial reference of IS in 2016 it was possible to quantify the relationship between IS and UHI. Based on this relation and knowledge of the future development areas from MP, it was possible to predict the future development of UHI in Prague.

The outputs confirmed that the development of UHI in the individual concentration zones of Prague was diverse. The large differences in population growth, the different amount of new build-up areas and the amount of vegetation caused no change in the *downtown*. Towards to the edge of city change grew and in the *outskirt* was extreme. The forecast has determined that this trend will continue into the future, as the largest spatial development will occur in the outer city and outskirt. This thesis created a missing study of Prague, which examined the impact of

urban development on the UHI with spatial references that were refined by data from the MP.

Keywords: NDVI, UTFVI, Impervious surfaces, Urbanization, Remote sensing

Abstrakt

Tato práce zkoumá vliv městského vývoje Prahy na *městský tepelný ostrov* (UHI) mezi lety 2002 a 2016 pomocí dálkového průzkumu země. Jako hlavní faktory jsou použity *normalizovaný diferenční vegetační index* (NDVI), autorem vytvořený *index zastavěnosti* (BI) a statistické údaje o počtech nově přistěhovalých lidí do jednotlivých městských zón. Pro kvantitativní interpretaci UHI byl použit *měrný index rozptylu tepelných polí* (UTFVI), který také popisuje míru ekologické zranitelnosti. *Povrchová teplota* (LST) byla interpretována dvěma způsoby pro lepší porovnání s ostatními faktory. První způsob je rozdíl mezi jednotlivými roky a druhý způsob je klasifikace jednotlivých let pomocí *přirozených zlomů* (Jenks) metody. Jednotlivé městské části zaznamenali rozdílný územní vývoj, proto autor použil rozdělení do čtyř koncentrických zón: *centrum*, *vnitřní město*, *vnější město* a *předměstí*. Snímek z roku 2002 byl pořízen družicí Landsat 7 (ETM+) a druhý snímek z roku 2016 byl pořízen družicí Landsat 8 (OLI and TIRS), oba v rozlišení 30-ti metrů. Pro porovnání bylo nutné určit vhodnou klasifikaci rozdílů jednotlivých let, z důvodu různých vlivů např. rozdílného vegetačního období, záměna povrchů atd. Pro vyšší přesnost výsledků byla z finálních výstupů před porovnáním vymazána orná půda. Pro rok 2016 byla provedena extrakce *nepropustných povrchů* (IS) pomocí kombinace BI a prostorových dat ze současného *Územního plánu* (MP) Prahy. Díky znalosti přesné prostorové reference IS v roce 2016 bylo možno kvantifikovat spojitost mezi IS a UHI. Na základě této spojitosti a znalosti plochy budoucí zástavby z MP bylo možno predikovat budoucí vývoj UHI v Praze.

Ve výstupech se potvrdilo, že vývoj UHI v jednotlivých koncentrických zónách Prahy byl různorodý. Velké rozdíly v migraci obyvatel, rozdílné množství nové zástavby a množství vegetace zapříčinili, že v centru města nebyla téměř žádná změna a směrem k okraji města tato změna narůstala až do extrému v předměstí Prahy. Predikce určila, že tento trend bude pokračovat i do budoucnosti, protože největší územní rozvoj zaznamenají okrajové části města *vnější město* a *předměstí*. Tato práce vytvořila chybějící studii Prahy, která zkoumala vliv městského rozvoje na UHI s prostorovou zpřesněnou referencí informacemi z MP.

Klíčová slova: NDVI, UTFVI, Nepropustné povrchy, Urbanizace, Dálkový průzkum

Chapters

1	INTRODUCTION	1
2	GOALS	3
3	LITERAL REVIEW	4
3.1	Urban development	4
3.1.1	Master plan	5
3.2	Urban heat island.....	6
3.2.1	Origin of UHI	8
3.2.2	Impacts of UHI.....	9
3.2.3	Mitigation of UHI.....	10
3.2.4	UHI in Prague.....	13
3.3	Remote sensing and UHI.....	15
3.3.1	Thermal remote sensing	15
3.3.2	Landsat 7 (ETM+) vs. Landsat 8 (OLI and TIRS).....	17
4	STUDY AREA	19
4.1	Geomorphological conditions	19
4.2	Climate	20
4.3	Urban development and population	21
5	METHODOLOGY	25
5.1	Selection of images	25
5.2	Pre-processing of images and data	27
5.2.1	Multispectral images pre-processing.....	27
5.2.2	Thermal images pre-processing	31
5.3	Processing of images and data.....	35
5.3.1	Extraction of impervious surfaces 2016.....	35
5.3.2	Estimation of future development areas	36

5.3.3	Mutual relation of IS and UHI	36
5.4	Analogy and prediction	37
5.4.1	Analogy between 2002-2016	38
5.4.2	Prediction based on MP	39
6	RESULTS	40
6.1	Downtown	40
6.2	Inner city	41
6.3	Outer city	41
6.4	Outskirt	42
7	DISCUSSION	43
8	CONCLUSION AND CONTRIBUTIONS	45
9	REFERENCES	46
9.1	Literature sources	46
9.2	Internet sources	48
10	LIST OF FIGURES	51
11	LIST OF TABLES	52
12	LIST OF APPENDIX	53
13	APPENDIX	55

LIST OF ABBREVIATIONS

BI - Build-up index

IS - Impervious surfaces

LST - Land surface temperature

MP - Master plan

NDVI - Normalized difference vegetation index

NDWI - Normalized difference water index

NDBI - Normalized difference build-up index

QUAC - Quick atmospheric correction

ROI - Region of interest

RS - Remote sensing

UHI - Urban heat island

UTFVI - Urban thermal field variance index

1 INTRODUCTION

The urbanization process has accelerated in the last few decades at a rapid pace. Approximately 54% of the world's population (UN 2014) lived in urban areas in 2014. The highest ratio was in North America (82%), Latin America and Caribbean (80%), and Europe (73%). Africa and Asia still had the majority of the population in rural areas (40% -48% living in urban areas). However, on these two continents the urbanization intensity was the highest, and it is predicted to reach even higher values. Prediction says that worldwide there will be approx. 2.5 billion new inhabitants in urban areas by 2050 and 90% of that will be in Asia and Africa. It will increase the share of worldwide urban population from 54% to 66% in 2050 (UN, 2016). Massive urbanization primarily affects Africa and Asia, where in most cases there are very various climatic conditions than in Europe. Population growth in cities will also be evident in Europe.

One of the major climatic phenomena that occurs in densely populated areas, is the urban heat island (UHI). This significant ascent in temperature over the surrounding landscape has a number of negative environmental impacts as well as prime impacts directly on health and comfort of people (U.S. Environmental Protection Agency, 2012). There are factors that affect this phenomenon and some of them may be artificially modified to suppress intensity of UHI. A number of studies investigate forms and appropriate use of mitigation measures (Gago, 2013; Gunawardena, 2017; Santamouris, 2012; U.S. Environmental Protection Agency, 2012). UHI monitoring is divided into surface UHI monitoring and atmospheric UHI. Atmospheric UHI is measured using fixed stations acquiring data by meteorological stations and mobile traverse, which is the measurement and generation of new data directly in the field. Surface UHI significantly influences the atmospheric UHI, and the surface type is measured by the remote sensing (RS) approach (US Environmental Protection Agency, 2012; UHI Assesment Manual, 2012). Surface UHI contains two different aspects, spatial (Imhoff, 2010) and time (Buyantuyev, 2010). A common element of UHI studies is a land use / land cover change, which is considered to be the basic factor of surface UHI origin (Bokaie, 2016; Singh, 2016; Son, 2016).

Czech Republic, as well as the capital city of Prague, has been experiencing increased frequency of extreme weather conditions associated with the changing climate in recent decades. The average annual air temperature is increasing (the current growth rate was about 0.3 °C per decade, a further increase of 1 °C is expected on our territory by 2030) and also the frequency of occurrence, intensity and duration of the period with extreme high temperatures (IPR, 2016). A study describing the UHI in Prague (CHMI and IPR, 2013; IPR, 2016) was developed, but none of them dealt with the growth and distribution of UHI in spatial contexts. The aim of this work is to map and analyse the development of surface UHI in Prague in the given time period by means of division into individual urban zones. Each urban zone has different characteristics of development and therefore the spatial development of the surface UHI should be different. There is also spatial planning documentation of Prague, which provides very accurate and valuable information on the current and future development of the city. The combination of remote sensing and extraction data from the Prague's Master plan (MP) documentation gives the possibility to predict where and to what extent the surface UHI can be expanded in the near future.

2 GOALS

Assess how urban development of Prague affected intensity of UHI in selected time period. Firstly is necessary to determine most suitable identifiers of urban development in Prague. Secondly is essential to adopt most conclusive way how to interpret these factors.

Determine relation of UHI and impervious surfaces (IS) in Prague. Based on that relation, predict future possible intensity of UHI. For estimation of future developable areas is crucial process data from current MP of Prague.

3 LITERAL REVIEW

In this chapter author provided theoretical background which was needed for elaboration of this thesis.

3.1 Urban development

The most accepted description and categorization of urban development according to Ouředníček (2000) is “*Theory of Stages of Urban Development*” described by Berg (1982) as: Urban development is described as directly dependent on social and economic level of society, mainly on changes in economic structure and income levels of inhabitants. Figure 1 shows, that theory is based on three fundamental stages of human society development, which are transformation of agricultural society into industrial, after into tertiary society and third stage represents society progress based on tertiary sector. Authors described following four stages of urban development:

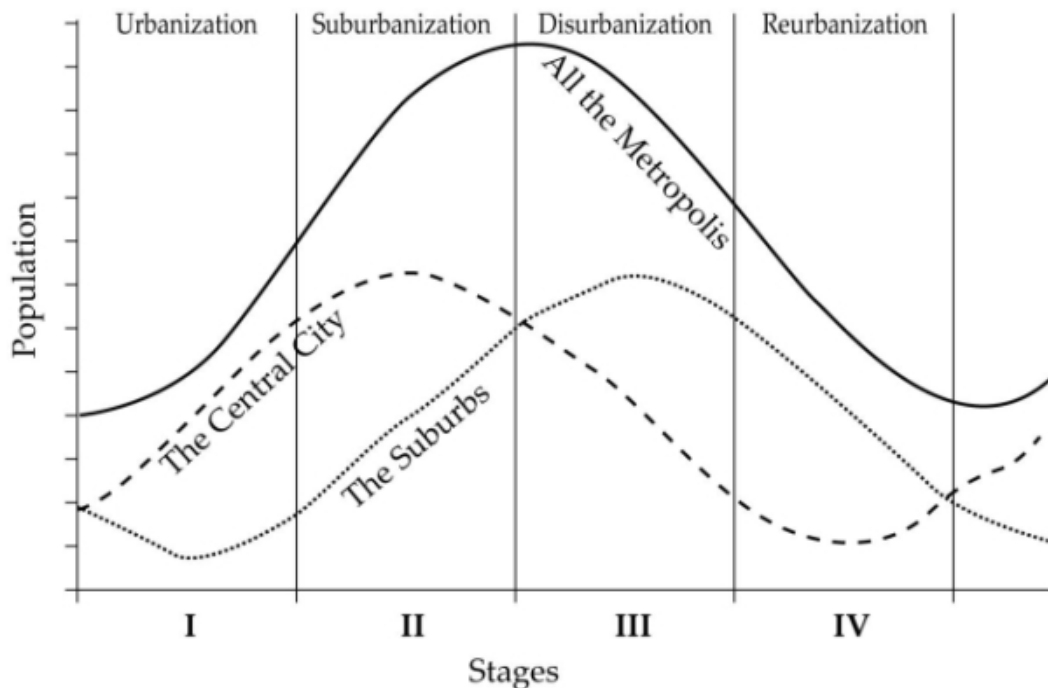


Figure 1: Metropolitan Development Model (Berg 1982).

Urbanisation is a first stage of development and it is created by surplus of labor power in agricultural areas, decline of wages in agriculture and industrial development in cities. These facts instigate a gradual allocation of people from rural area to cities. People settled mainly in the central areas of cities, near the industrial

areas which led to their low transport mobility. This process led to concentration of the population and expansion of industrial and residential areas of the cities.

Suburbanization is a continuation of the urban development in industrial age, when qualitative changes started emerge, especially housing and transportation. Population moved more towards outskirts of city, thanks to better interconnection of suburbs and city. Simultaneously, industrial facilities moved to more strategic locations but still with good transport accessibility. Separation between the place of residence and workplace on work class level started. Urban agglomerations are formed, with populations concentrated along major transport routes around the city.

On the other hand, processes mentioned above brought also negative effects, related to unbearable overloading of city transportation system which leads to decline of permeability of city itself. Administration and retail print out residential areas and many services is moving with residents to regions beyond borders of city. Decline of population is noticeable in city core and also suburbs, meanwhile originally countryside regions in broader background of city are transforming to settlements of higher intensity. This phenomenon is called inter-urban decentralization, in other word desurbanization.

Berg (1982) provides alternative in form of process reurbanisation, which is connected with city effort for revitalization of city core by doing this “*Programs to improve the image of the city, rehabilitate the residential environment, improve the traffic situation, create pedestrian zones and improve social infrastructure.*” (Berg, 1982). As main feature could be pointed need of approximation of residential areas to work places. This effort is not just on municipal level, but it is supported also on national level by Czech policy of spatial development (PÚR ČR 2015) via enforcement of polycentric development. Lower level of spatial planning documents called MP is used on municipal level.

3.1.1 Master plan

Paragraph no. 3, § 43, SZ 225/2017 sb. Says: “*Master plan in contexts and details of municipality specifies and develops the objectives and tasks of spatial planning in accordance with the principles of spatial development of the region and with the policy of spatial development.*”(Translated from Czech original by author)

MP is most important document with normative character on local level. It creates rules for changes in usage of areas and permitting new structures. Some requirements on MP can result from program of municipality development but also directly from public and experts. (Maier, 2012) MP is legally binding document on municipality level and is required to comply with superior spatial planning documentation. In general, it is main tool which municipalities have for spatial development planning. When MP is officially required or changed, it is obligatory for all entities in territory fulfil all conditions which MP contains in case of new development. Presence of development which already happened before current MP, can't be affected based on principle that the law can't be enforced retroactively.

Paragraph no. 1, § 43, SZ 225/2017 sb. Says: *“Master plan provides basic conception of development of the municipality territory, protection of its values, its area and spatial layout (furthermore “urban conception”), landscape design and public infrastructure conception; define buildable territory, areas and corridors, especially buildable areas, areas for changes in landscape and areas defined for change of already existing build-up areas, for recovery or reuse of degraded areas (furthermore “redevelopment areas”), for publicly beneficial structures, for publicly beneficial measures and for spatial reserves and define conditions pro usage of these areas and corridors.”*(Translated from Czech original by author).

MP defines functional zones with very detailed conditions for new development, which is very important feature for this work. MP also including spatial regulations, whose define especially maximal capacity and intensity of new development. This type of regulation is defined differently for stabilized areas, for development areas, for transformation areas and non-development areas. Main types of spatial regulations are coefficient of height (maximal amount of floors), coefficient of greenery (minimal amount of green area) (IPR Praha).

3.2 Urban heat island

“One of the best known effects of the influence of the urban environment on its climate is the urban heat island effect. This is the phenomenon that the urban air temperature is higher than that of the surrounding rural environment” (Kleerekoper, 2012).

The heat generated by and contained in an area could be given by surface energy balance as equation:

$$Q^* + Q_F = Q_H + Q_E + \Delta Q_S + \Delta Q_A \quad (1)$$

where, Q^* is the net all wave radiation, Q_F is anthropogenic heat release, Q_H is the turbulent sensible heat flux, Q_E is the turbulent latent heat flux, ΔQ_S is the net sensible heat storage and ΔQ_A is the net heat advection (Rizwan, 2007).

In general there are surface and atmospheric types of UHI. These two types differ in many ways, in following Table no.1 we can see major differences:

Table 1: Basic Characteristics of Surface and Atmospheric UHIs (U.S. Environmental Protection Agency, 2012).

Feature	Surface UHI	Atmospheric UHI
Temporal Development	<ul style="list-style-type: none"> • Present at all times of the day and night • Most intense during the day and in the summer 	<ul style="list-style-type: none"> • May be small or non-existent during the day • Most intense at night or predawn and in the winter
Peak Intensity (Most intense UHI conditions)	<ul style="list-style-type: none"> • More spatial and temporal variation: <ul style="list-style-type: none"> ▪ Day: 18 to 27°F (10 to 15°C) ▪ Night: 9 to 18°F (5 to 10°C) 	<ul style="list-style-type: none"> • Less variation: <ul style="list-style-type: none"> ▪ Day: -1.8 to 5.4°F (-1 to 3°C) ▪ Night: 12.6 to 21.6°F (7 to 12°C)
Typical Identification Method	<ul style="list-style-type: none"> • Indirect measurement: <ul style="list-style-type: none"> ▪ Remote sensing 	<ul style="list-style-type: none"> • Direct measurement: <ul style="list-style-type: none"> ▪ Fixed weather stations ▪ Mobile traverses
Typical Depiction	<ul style="list-style-type: none"> • Thermal image 	<ul style="list-style-type: none"> • Isotherm map • Temperature graph

“A distinction between surface and atmospheric urban heat islands has to be made. These two differ in the ways they are formed, the techniques used to identify and measure them, their impacts, and to some degree, the methods available to mitigate them. Surface urban heat islands are typically present day and night, but tend to be strongest during the day when the sun is shining. Atmospheric UHI are often weak during the late morning and throughout the day and become more pronounced after sunset due to the slow release of heat from urban structures. The timing of this peak, however, depends on the properties of urban and rural surfaces, the season, and prevailing weather conditions.” (Hove, 2011)

For the selection of images to analyse is key fact, that surface UHI has peak values during day time in summer. Also is very important to take into consideration prevailing meteorological conditions and urban surfaces.

3.2.1 Origin of UHI

Relation of city and climate is significant, because climate has significant effect on the way how city space is used and type of buildings. On the other hand city influences its climate. *“On the large scale the city as a whole modifies the regional climate conditions, which result in differences between the city and its surrounding (rural area in cloud cover, precipitation, solar irradiation, air temperature and wind speed. On a smaller scale, the geometry, spacing and orientation of buildings and outdoor spaces strongly influence the microclimate in the city.”* (Kleerekoper, 2012)

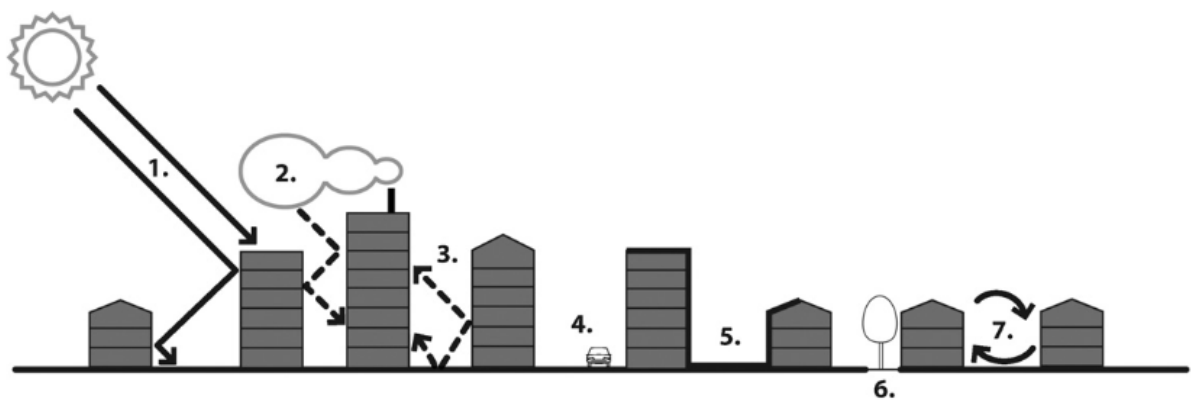


Figure 2: Causes of UHI (Kleerekoper, 2012).

UHI has following causes according to Kleerekoper (2012) in Figure 2:

- 1) *“Absorption of short-wave radiation from the sun in low albedo (reflection) materials and trapping by multiple reflections between buildings and street surface.*
- 2) *Air pollution in the urban atmosphere absorbs and re-emits long-wave radiation to the urban environment.*
- 3) *Obstruction of the sky by buildings results in a decreased long-wave radiation heat loss from street canyons. The heat is intercepted by the obstructing surfaces, and absorbed or radiated back to the urban tissue.*
- 4) *Anthropogenic heat is released by combustion processes, such as traffic, space heating and industries.*

- 5) *Increased heat storage by building materials with large thermal admittance. Furthermore, cities have a larger surface area compared to rural areas and therefore more heat can be stored.*
- 6) *The evaporation from urban areas is decreased because of 'waterproofed surfaces' – less permeable materials, and less vegetation compared to rural areas. As a consequence, more energy is put into sensible heat and less into latent heat.*
- 7) *The turbulent heat transport from within streets is decreased by a reduction of wind speed. See Fig. 1 for illustrations."*

Main source of heat causing UHI is sun radiation which is accumulated by urban mass and area. Low level of albedo allows accumulation but higher albedo could also increase UHI intensity when it's reflecting radiation towards another structures. Urban geometry should be designed regarded to specific geomorphological and meteorological conditions of location. Increasing amount of IS is decreasing evaporation from urban areas which leads increase of latent heat.

3.2.2 Impacts of UHI

According to U.S. Environmental Protection Agency (2012) increased temperatures from UHI, especially during summer have significant effects for the local environment and quality of life. Some impacts are positive, for example lengthening the plant-growing season, but most of impacts are negative such as:

1) Increased energy consumption

Especially increased summer temperatures in cities increase energy consumption due to higher need for cooling and it adds pressure to the electricity grid during peak periods of demand, which are generally during summer, hot weekdays. Energy demand is increased by 1,5 to 2 % for every 0,6^oC increase of summer temperature during the peak.

2) Elevated emissions of air pollutants and greenhouse gases

Increased energy demand generally causes higher levels of air pollution and greenhouse gas emissions. This impact is directly related on the source of energy. For example, if the main source of electricity are fossil fuels, than there will be increased level of pollutants in the air which are harmful to human health and

contribute to complex air quality problems. On the other hand this impact could be mitigated at the source by using of green energy.

3) Compromised human health and comfort

Most vulnerable are children, older adults, and those with existing health conditions, because increased daytime surface temperatures, reduced night time cooling, and higher air pollution levels are associated with UHI can cause significant negative effects on human health.

4) Impaired water quality

Surface UHI degrades water quality by thermal pollution. IS reach higher temperatures than air and transfer this excess heat to storm water. This heated water generally drains into the storm sewer and is released to water bodies, where the fragile ecosystem is affected by higher temperatures.

Impacts overview according Voogt (2004) is following:

- *“human comfort: **positive** (winter), **negative** (summer),*
- *energy use: **positive** (winter), **negative** (summer),*
- *air pollution: **negative**,*
- *water use: **negative**,*
- *biological activity (e.g., growing season length): **positive**,*
- *ice and snow: **positive**.”*

As it is mentioned above, there are also positive effects of UHI. During planning and also designing of urban areas and structures is necessary to consider all circumstances and take advantage of UHI when it is possible, instead of just eliminating this process.

3.2.3 Mitigation of UHI

Mitigation measures could be divided into two main categories and described as following (Gago, 2013):

1) Planning strategies for mitigation of the heat island effect (1): Green spaces and trees, albedo and pavements

a) Parks and green areas

Combined effects of evapotranspiration and shading causes a significant decrease in temperature, therefore this combination of effects is described as a cool islands in the city. General consensus of various studies which analysed the temperature in parks and beneath trees was that green spaces were cooler than spaces without any greenery.

“All types of greenspaces provide varying ecosystem services to the urban environment including; reduced surface runoff, flood relief, sustainable drainage, general aesthetic and wellbeing enhancements and the modification of local microclimates.”(Gunawardena, 2017)

b) Trees and vegetation

“The presence of vegetation can generate localized cooling, a phenomenon known as “island of amelioration”, which is the opposite of the UHI phenomenon.” (Santos, 2017)

Reduction of energy consumption caused by vegetation and tree shade could

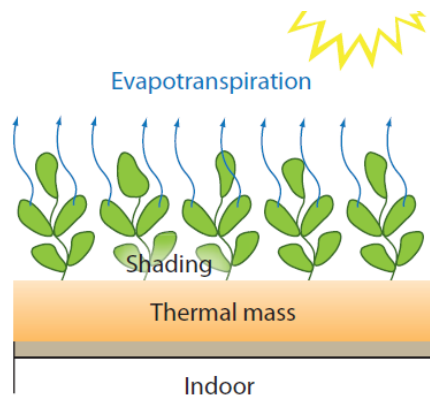


Figure 3: Evapotranspiration and Shading on a Green Roof (U.S. Environmental Protection Agency, 2012).

be up to 10% in cooling of buildings. Highest effect in cooling of buildings has 100% greenery coverage from vertical greenery systems. Vegetation also has negative effects for urban microclimate in cold climates, dense shade, as in conifers, can increase heating costs up to 21% but shade from leafless deciduous trees is less important. Because effect of vegetation could be negative and positive it is necessary to have an in-depth knowledge of the plant species as well as of the local climate.

Factors which can affect significantly energy consumption of nearby buildings are site climate, the tree species at the location and number of trees in relation to the surface area.

c) Green roofs

Green roofs are feasible solutions which improves building energy performance as well as the environmental conditions of the surroundings. Green roofs also leads to

significant reduction in the rainwater input in the sewage system during rainfalls that helps to stem the rising risk of flooding in many cities. Reduction of rainwater outcome could be up to 100%, due to evaporation and usage of rainwater for toilet flushing in buildings. Figure 3 shows structure and functions of green roofs.

d) Albedo

“Solar reflectance, or albedo, is the percentage of solar energy reflected by a surface. Most research on cool pavements has focused on this property, and it is the main determinant of a material’s maximum surface temperature.” (U.S. Environmental Protection Agency, 2012)

The incident solar radiation on urban surfaces is transformed into sensible heat, which accumulates in forms of large mass (roofs, building surfaces, streets etc.). Intensity depends on the percentage of surfaces visible to the sky and on the characteristics of materials such as albedo, emissivity etc.

According Taha (1995), usage of high-albedo materials decreased the solar radiation absorbed by buildings and urban structures. Result was that air temperatures on summer days can be lowered up to 4°C, by increasing the surface albedo by 40% in a mid-latitude warm climate.

e) Pavements

Sidewalks could occupy up to 23% of area in rectangular urban design and have important role in temperature balance. Three important factors according Gago (2013) are:

- *“the horizontal surface exposed to solar radiation,*
- *the absorptance (ratio of the amount of radiation absorbed by a surface to the total radiation incident upon it,*
- *the generally high thermal capacity of the materials used.”*

Doulos (2003) in his study analysed 93 pavement materials, commonly used in outdoor urban spaces for decreasing temperature. Main difference in daily mean temperatures of materials was albedo factor. “Hot materials” tend to absorb more solar radiation than smooth, light-colored and flat surfaces of “cool materials”. Result is that hot materials are suitable for cold climate and cold materials are suitable for hot climate.

2) Planning strategies for mitigation of the heat island effect (I1): Urban design

Formation of UHI is affected also by density of urban structures in city, because it has effect on absorption of solar energy and the formation of wind streams. Optimal designs can reduce energy consumption and CO₂ emissions, which can counteract the negative effects of the heat island.

Lariviere (1999) studied how electricity consumption is affected by a series of variables of all kind related to features of urban structures, urban design, types of heating, and even standard of culture life. Only variable whose increase led to reduction of electricity consumption was density of urban structure. Energy performance of building can vary up to 10% depending on urban design.

3.2.4 UHI in Prague

According to study of ČHMÚ and IPR (2013) is UHI in Prague on lower level of intensity. Study processed statistics from 1961 to 2012 with the following outcomes:

- annual average UHI intensity (1961 – 2012): 2,2 °C,
- the peak intensity of UHI in June and July is 2,4 °C and the lowest in September 1,9 °C,
- the main difference in minimum temperatures,
- the larger UHI intensity during anticyclone situations with prevailing NE-N winds
- the larger the cloudiness the smaller UHI is.

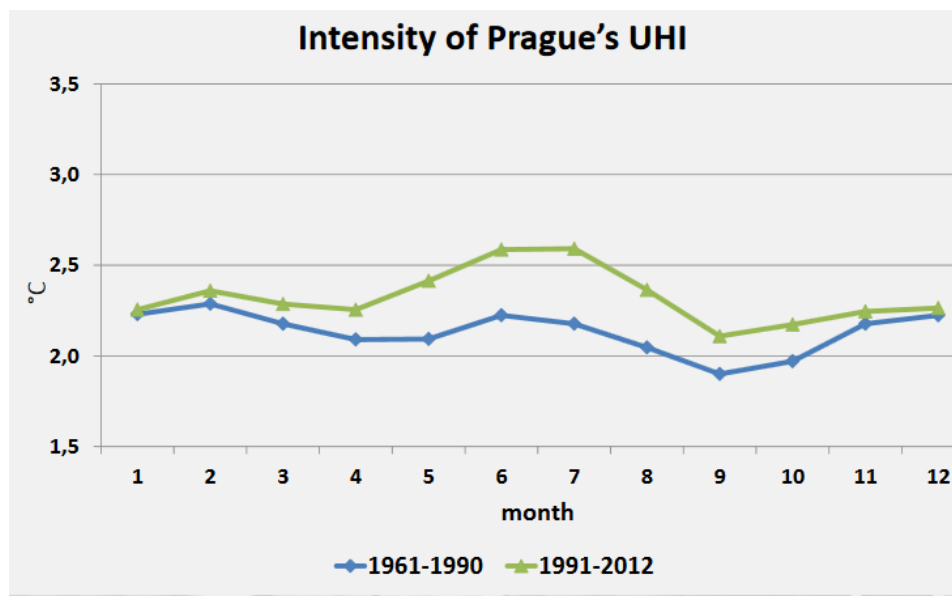


Figure 4: Intensity of Prague's UHI (ČHMÚ and IPR, 2013)

UHI intensity is according to Figure 4 and 5 in trend of growth, when during the summer months the difference between two compared periods is up to 0,8 °C due to city enlargement (Czech Hydrometeorological Institute and IPR, 2013). The Figure 5 shows spatial distribution of UHI in Prague. Highest intensity is downtown area and north part of Prague. In regular buffers around warmest central zone it is spreading to the further edges with decreasing intensity.

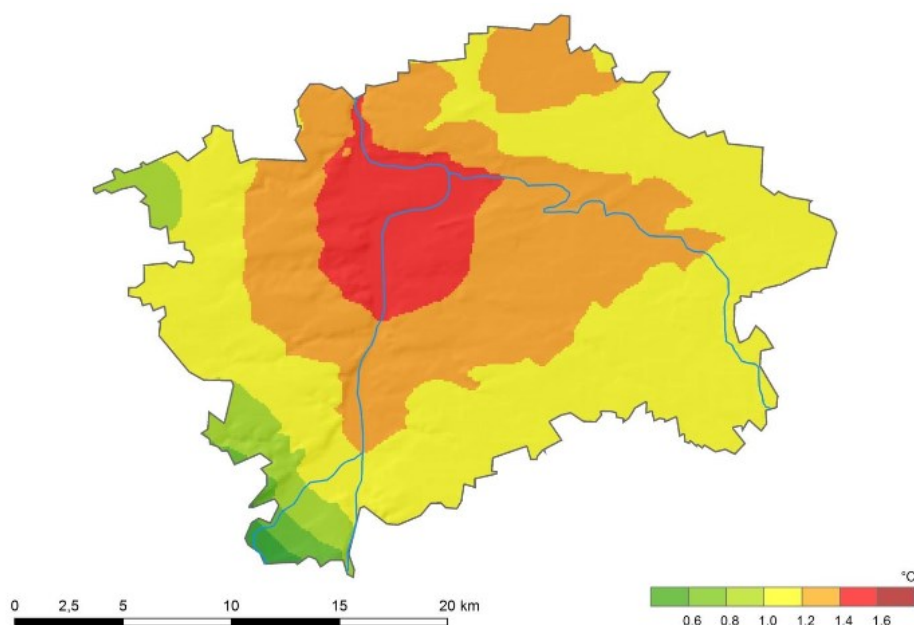


Figure 5: Change of average daily T_{\min} between 2001-2001 and 1961-1970 (ČHMÚ and IPR, 2013)

3.3 Remote sensing and UHI

UHI is traditionally analyzed based on land surface temperature (LST) data, collected via observation points. Since 1960, it is possible to use high-resolution earth monitoring satellites which led to RS technology become widely used tool for measuring LST and obtainment of another UHI basic data. (SANTOS, 2017)

Many studies demonstrated the wide and versatile applications of RS for determining surface temperature according to Rizwan (2008).

“The surface temperature is of prime importance to the study of urban climatology. It modulates the air temperature of the lowest layers of the urban atmosphere, is central to the energy balance of the surface, helps to determine the internal climates of buildings and affects the energy exchanges that affect the comfort of city dwellers.” (Voogt, 2002)

RS is very effective for collecting and also analysing of LST in bigger areas. There is no other tool which can work in same extend of data. Combination with fact, that surface temperature is most important factor for studying urban climatology is clear importance using of RS for studying of UHI.

3.3.1 Thermal remote sensing

“Thermal remote sensing is the branch of remote sensing that deals with the acquisition, processing and interpretation of data acquired primarily in the thermal infrared region of the electromagnetic spectrum. In thermal remote sensing we measure the radiations 'emitted' from the surface of the target, as opposed to optical remote sensing where we measure the radiations 'reflected' by the target under consideration.”(Prakash, 2000)

Every object with temperature higher than 0 °K emits electro-magnetic radiation, according to Zemek (2013). Amount and spectral content of emitted energy depends on temperature of object and its emissivity. For RS is major thermal feature of objects its emissivity, which could be described as a radiation of thermal radiation by the object in comparison to thermal radiation emitted by absolutely black object with same temperature. Assuming that temperature of observed objects on earth surface is between 270 – 330 °K and object is captured in a perpendicular projection, than we assume that emissivity basically depends only on wavelength. It

is crucial to take account an actual weather, seasonal and daily influences, which can significantly affecting temperature exchange on earth surface.

Thermal manifestation of surface can be described in two ways. Firstly it is thermodynamic state of object (its surface) and secondly it is also consequence of energetic transformations on surface of object. Surface temperature changes in nature are based on changes of whole complex of radiation changes between surface, environment and heat conduction. Energy which is incoming to system applies here and also amount of energy which leaves from the system.

3.3.1.1 Infrared wavelength

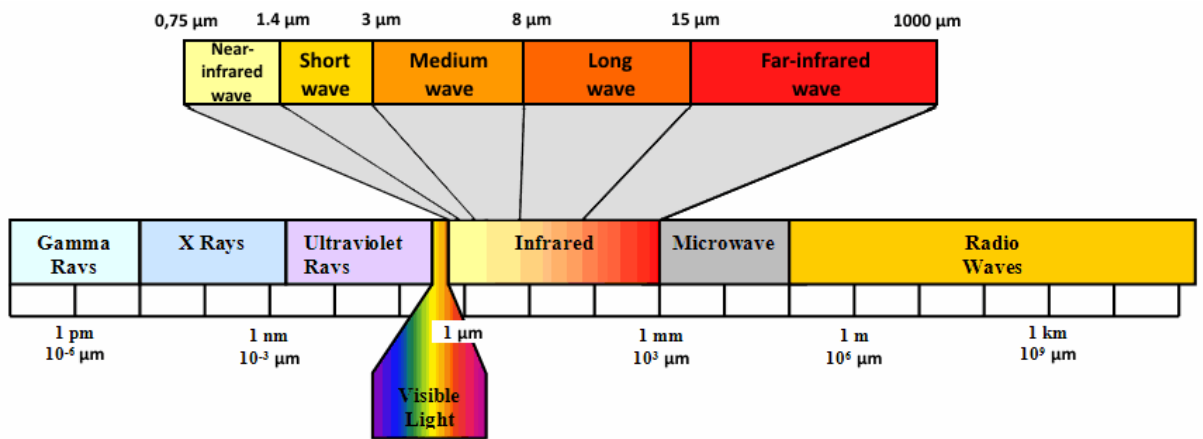


Figure 6: Infrared portion of the electromagnetic spectrum (Optics for hire).

So called “light” is just electromagnetic radiation which we can see on our own eyes. But the visible light is just small portion of full electromagnetic spectrum in Fig.6. gamma rays, x rays, ultraviolet, infrared, microwave and radio waves are all forms of electromagnetic radiation of varying energy.

For purpose of this thesis we will focus on infrared section of electromagnetic spectrum. Infrared region covers wavelength range from approx. 0.7 μm to 100 μm which is more than 100 times wider than visible section. Infrared region is divided into two categories based on their properties:

Reflected IR is used by RS in similar ways as the visible portion of electromagnetic spectrum. The reflected IR covers wavelengths from approx. 0.7 μm to 3 μm.

Thermal IR (emitted) differs a lot from visible part of electromagnetic spectrum and reflected IR, because it is radiation which is emitted from the surface of Earth in

a form of heat. The thermal IR covers wavelengths from approx. 3.0 μm to 100 μm (Natural Resources Canada).

3.3.2 Landsat 7 (ETM+) vs. Landsat 8 (OLI and TIRS)

Table 2 shows, that Landsat ETM+ have eight bands in total. Seven of them has resolution of 30 metres and one with resolution of 15 metres. The approximate scene size is 170 km north-south by 183 km eas-west (U.S. Geological Survey).

Table 2: Landsat Enhanced Thematic Mapper Plus (ETM+) (U.S. Geological Survey).

Landsat 7 Enhanced Thematic Mapper Plus (ETM+)	Bands	Wavelength (micrometers)	Resolution (meters)
	Band 1 - Blue	0.45-0.52	30
	Band 2 - Green	0.52-0.60	30
	Band 3 - Red	0.63-0.69	30
	Band 4 - Near Infrared (NIR)	0.77-0.90	30
	Band 5 - Shortwave Infrared (SWIR) 1	1.55-1.75	30
	Band 6 - Thermal	10.40-12.50	60 * (30)
	Band 7 - Shortwave Infrared (SWIR) 2	2.09-2.35	30
	Band 8 - Panchromatic	.52-.90	15

* ETM+ Band 6 is acquired at 60-meter resolution, but products are resampled to 30-meter pixels.

Table 3 shows, that OLI and TIRS images contain eleven bands in total, ten with resolution of 30 metres and one with resolution if 15 metres. Thermal bands no. 10 and no. 11 are useful in providing more accurate surface temperatures and are collected at 100 meters. The approximate scene size is 170 km north-south by 183 km eas-west (U.S. Geological Survey).

Table 3: Landsat 8 Operational Land Imager (OLI) and Thermal Infrared Sensor (TIRS) (U.S. Geological Survey).

Landsat 8 Operational Land Imager (OLI) and Thermal Infrared Sensor (TIRS)	Bands	Wavelength (micrometers)	Resolution (meters)
	Band 1 - Ultra Blue (coastal/aerosol)	0.435 - 0.451	30
	Band 2 - Blue	0.452 - 0.512	30
	Band 3 - Green	0.533 - 0.590	30
	Band 4 - Red	0.636 - 0.673	30
	Band 5 - Near Infrared (NIR)	0.851 - 0.879	30
	Band 6 - Shortwave Infrared (SWIR) 1	1.566 - 1.651	30
	Band 7 - Shortwave Infrared (SWIR) 2	2.107 - 2.294	30
	Band 8 - Panchromatic	0.503 - 0.676	15
	Band 9 - Cirrus	1.363 - 1.384	30
	Band 10 - Thermal Infrared (TIRS) 1	10.60 - 11.19	100 * (30)
	Band 11 - Thermal Infrared (TIRS) 2	11.50 - 12.51	100 * (30)

* TIRS bands are acquired at 100 meter resolution, but are resampled to 30 meter in delivered data product.

Figure 7 clearly shows, that OLI sensors with two additional spectral bands and narrower band width is significant advantage for application which requiring finer narrow bands more so the development of spectral indexes for the various applications of Landsat data (Mwaniki, 2015).

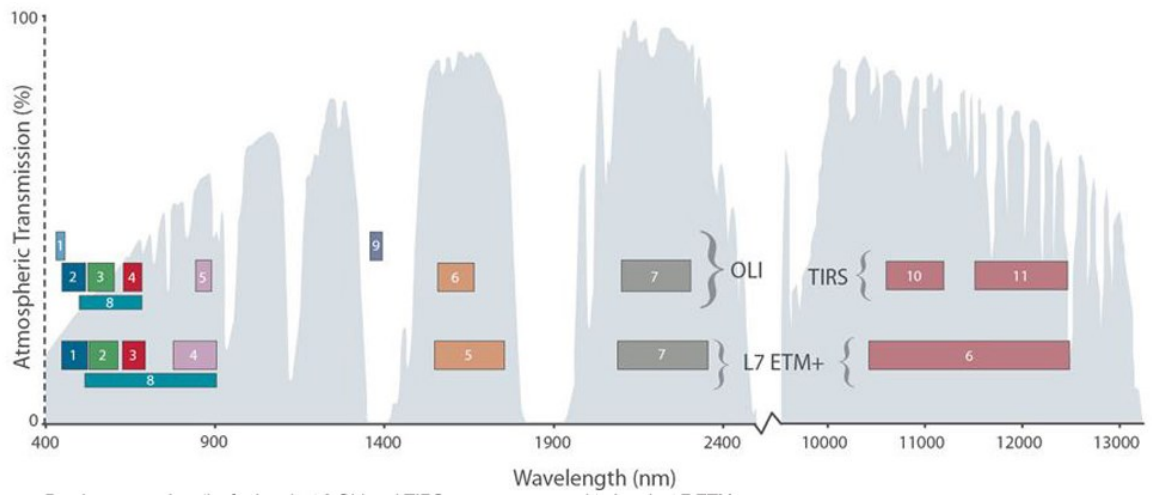


Figure 7: Bandpass wavelengths for Landsat 8 OLI and TIRS sensor, compared to Landsat 7 ETM+ sensor (U.S. Geological Survey).

4 STUDY AREA

Prague is capital and currently the biggest city of Czech Republic and 15th largest city of European Union. Lays slightly on the north from center of Bohemia on river Vltava, inside of Central Bohemian Region, for which is the administrative center, but as but as a separate region is not part of it.

4.1 Geomorphological conditions

Prague lays slightly north from central part of Bohemia region and extents in the valley of river Vltava and its tributaries. Their erosive activity modeled a rugged relief with the lowest point in Vltava river at Suchdol (177 m. a. s. l.), the highest peak is Teleček between Sobín and Chrást'any (399 m. a. s. l.) and in the center is a distinctive peak Petřín (327 m. a. s. l.).

Majority of the city's total area belongs to the Prague Platform, and only a smaller part in the northeast belongs to the Central Bohemian Board. At the very southern part of the town, two other units penetrate their spurs, while fluvial soil in estuary of river Berounka belongs to the Hořovice Upland, while the Brda Highland reaches its highest end between Baně and Točná to the right bank of Vltava river. In Figure 8 we can see how lowest part in general is city downtown and edges of city have higher elevation, which might cause longer staying of heat in the lower parts of city.



Figure 8: Geographical map of the Capital city of Prague (ČÚZK).

4.2 Climate

The climatic conditions of the particular area are determined by the characteristic weather regime, which determines the energy balance, the circulation of the atmosphere, the character of the active surface and the influence of anthropogenic activity. The Czech Republic is situated in the temperate zone of the northern hemisphere in the middle of Europe, where the influence of the Gulf Stream is still one of the most important factors. For our territory it is characterized by a generally favourable, mild, humid climate of oceanic character and alternation of four seasons (ÚAP Hl. m. Prahy, 2008)

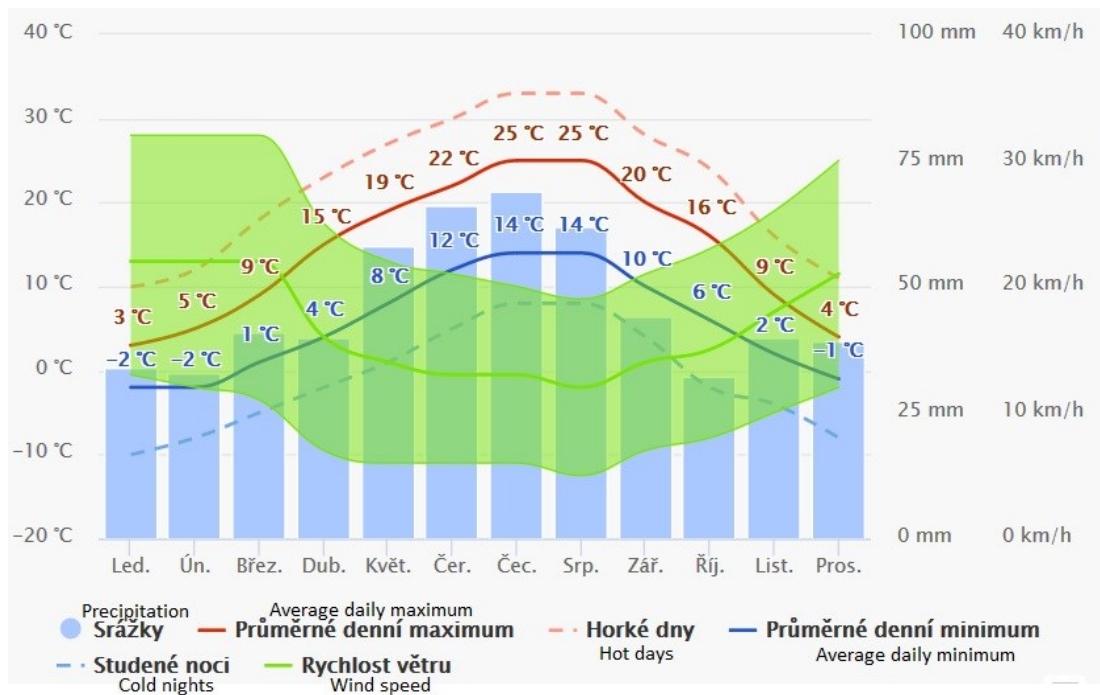


Figure 9: Average precipitation total in Prague (Meteo Blue).

Prague territory lays climatologically on the boundary between a region with warm, dry and mild winters and slightly warm, dry, mostly mild winters. The long-term annual average air temperature (1951-1990) varies from 9.9 °C in the center of Prague (Klementinum) to 7.9 °C in the highest positions on the outskirts of the city (Ruzyne). In the coldest month of January, the average daily temperature is 1 °C, nighttime -3 °C. In the warmest month of July, the average daily temperature is 24 °C, the night is 13 °C. Annually, there are about 100 freezing days and 30 cold days. Relative humidity is between 65% and 90% throughout the year. The Figure 9 shows that three warmest month are June – August with combination with lower wind speed and higher level of precipitation.

4.3 Urban development and population

Suburbanization process was stopped during communist times by state's central planning urbanization policies, which brought investments to urban center and high density, high-rise housing estates built at the edges of the Prague. Concentration of urban development in Prague's core became a dominant pattern of metropolitan growth of that time. After 1989, the re-establishment of a capitalist system based on the principles of decentralized decision making within free market

economy and democratic political system brought radical internal transformations to social practices and social structures (Sýkora, 2012).

Prague is not an internally homogeneous spatial unit, and individual municipalities are undergoing a very different population development. Prague can be divided into four concentric zones according to Ouředníček (2012):

- 1) downtown corresponds approximately historic boundaries of medieval Prague,
- 2) inner city represents outskirts and residential areas related to urban development in during 19th century and beginning of 20th century (approximately area of First Republic Great Prague)
- 3) outer city in which concentrates mostly socialist panel constructions
- 4) Outskirt represented by previously independent residences, which were connected to Prague, but they are not part of compact city development (Figure 10).

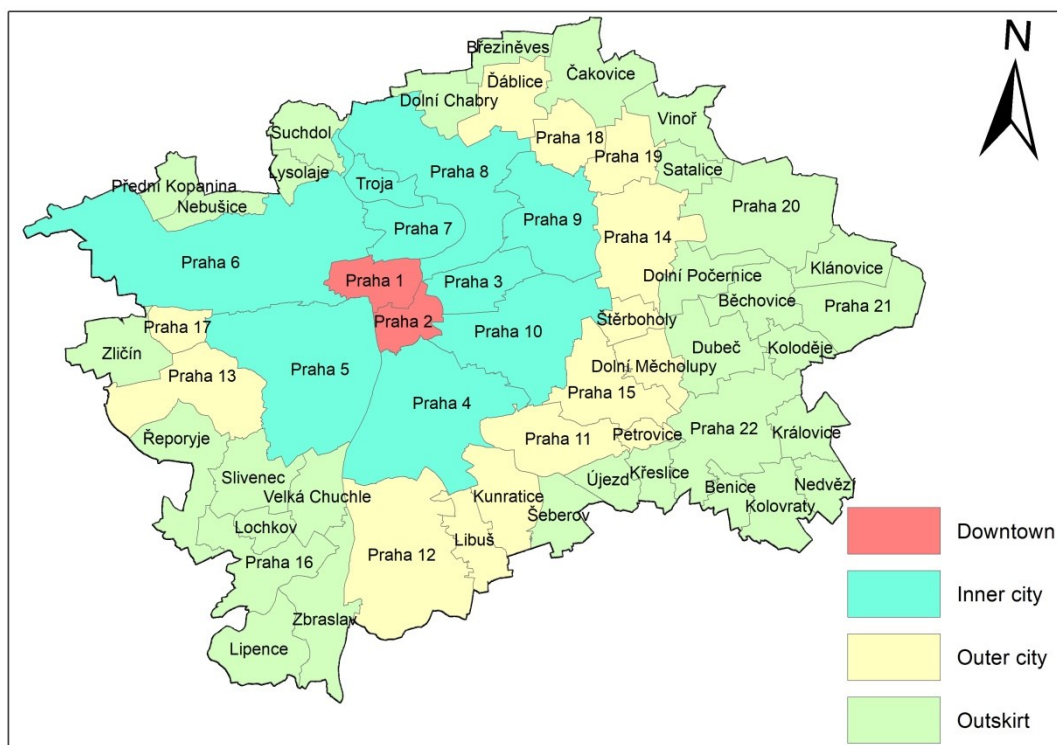


Figure 10: Division into concentric zones (Author, based on Ouředníček, 2012).

Basic data and information about population in particular Prague's zones is in Table 4 and changes between the years are in Table 5. Differentiation of the

population development within Prague is very clearly illustrated by the actual comparison of the population in individual urban zones at the beginning and the end of the monitored period. The population of Prague as a whole grew by 14.55% between 1991 and 2016. At the same time, the downtown lost 24.45% and the inner city lost 4.59 %. On the contrary regions with population growth are the outer city with 23,17%, the outskirts with 72,61% and the surroundings of Prague with 77,15%.

Table 5 clearly shows moments of sub-phase and break-even moments in population growth of individual urban zones. Downtown and inner city significantly lose their population by 2005. After this year, downtown is stagnating and the inner city is experiencing a significant increase between the years 2005-2009, then the increase is declining. The outer city as the only part grew till 1995 due to the completion of some prefab estates (Ouředníček, 2012). In terms of population growth, the most dynamic change is recorded by outskirts and surroundings. While in the first half of the 1990s the population growth of these areas did not show significant dynamics, from the second half of the 1990s they have recorded large and increasing population growths. After the year 2000, other urban zones are gradually added to the urban zones with strong population growth. Positive population growth spreads from the edges to the center of the city. The outskirts has been growing since 1991, the outer city since 2000, the inner city since 2005 and the downtown has been stagnating since 2005. Population growth over the last two time periods is absolutely exceptional, with the numbers of new inhabitants reaching high amounts in nearly all areas. The fastest growing zone is surroundings, where its gain has more than doubled over the last three periods, and is clearly the most dynamic region, but all zones are in trend of decreasing of growth in last period.

Table 4: Population in Prague 1991 - 2016 (Author, based on Czech Statistical Office)

Population						
Zones	1991	1995	2000	2005	2009	2016
Downtown	104 463	95 325	86 675	79 877	79 891	78 922
Inner city	737 514	714 267	687 339	671 993	697 898	703 681
Outer city	292 361	319 144	321 774	329 327	349 744	360 103
Outskirt	79 836	81 119	85 338	100 413	121 493	137 802
Surroundings*	176 188	176 800	187 156	212 687	257 946	312 122
Whole Prague area	1 390 362	1 386 655	1 368 282	1 394 297	1 506 972	1 592 630

* Contains Prague-East and Prague-West

Table 5: Change of population 1991 - 2016 (Author, based on ČSÚ)

Change of population					
Zones	1991-1995 (4 y)	1995-2000 (5y)	2000-2005 (5y)	2005-2009 (4y)	2009-2016 (7y)
Downtown	-9 138	-8 650	-6 798	14	-969
Inner city	-23 247	-26 928	-15 346	25 905	5 783
Outer city	26 783	2 630	7 553	20 417	10 359
Outskirt	1 283	4 219	15 075	21 080	16 309
Surroundings*	612	10 356	25 531	45 259	54 176
Whole Prague area	-3 707	-18 373	26 015	112 675	85 658

* Contains Prague-East and Prague-West

5 METHODOLOGY

In this chapter author provided detailed description of all processes which were done in practical part of thesis.

5.1 Selection of images

Key factor for creation of UHI are higher temperatures for several days in row without any rain. In Figure 9, we can see that highest temperatures are in July and August and on second position is June. These three months were selected for further research of most suitable images from two different time periods at least ten years between them. Combination of high temperatures and low wind speed is most suitable for identifying UHI. High level of precipitation is least wanted, but with the right selection of images author avoided time periods when rain occurred.

Images from two different years were compared, so it had been necessary to find images from same sensor or at least from two comparable ones. As most suitable days for comparison, were selected 19th of June 2002 and 24th of June 2016. As Table 6 shows, both images were taken by Landsat class of sensors, image from 2002 by Landsat 7 and image from 2016 by Landsat 8. These two particular days fulfil various conditions for selection:

- Similar part of year and month
- Similar meteorological conditions without precipitation
- Almost no cloud coverage on images
- Images acquired by comparable sensors

Table 6: Used data (Author).

Data used	Date of aquisition	Source
Landsat ETM +	19th of June 2002	https://earthexplorer.usgs.gov/
Landsat OLI and TIRS	24th of June 2016	

Table 7 shows, that both selected dates had almost identical temperature gains in 2 last days before images were acquired. Combination of these two images is the best match of all conditions mentioned above, which author was able to obtained.

Table 7: Overview of meteorological conditions of selected time periods (Author).

Date	Cloudiness	Average day temperature (°C) *	Average night temperature (°C) *	Average length of sunshine (Hours) *
2002				
17.6.	Clear sky	27,95	12,85	13,6
18.6.	Clear sky	30,38	16,45	14,2
19.6.	Clear sky	31,45	18,13	13,3
2016				
22.06.	Partly cloudy	27,05	14,78	8,1
23.06.	Clear sky	30,88	16,18	15,5
24.06.	Clear sky	32,53	18,93	14,4

*Data is averaged from four meteorological stations in Prague, which are slightly different in particular years. For 2002 were used Praha – Kbely, Praha – Klementinum, Praha – Libuš and Praha – Ruzyně. For 2016, were used Praha – Kbely, Praha – Karlov, Praha – Libuš, Praha – Ruzyně.

5.2 Pre-processing of images and data

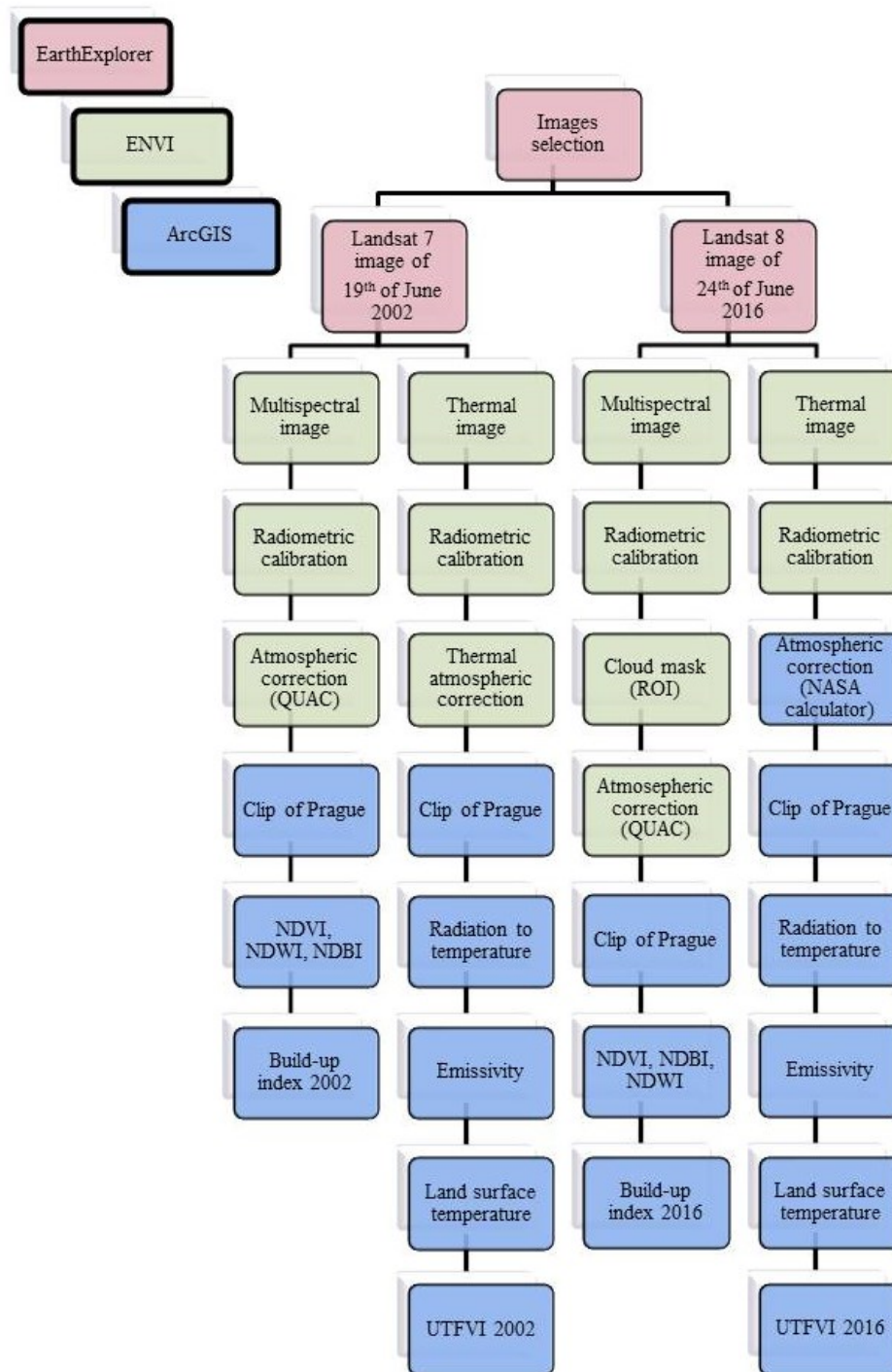


Figure 11: Workflow pre-processing of images and data (Author).

5.2.1 Multispectral images pre-processing

All steps of multispectral images pre-processing were made in several different software as Figure 11 shows. Firstly images were selected and downloaded

by USGS Earth Explorer and after were modified in ENVI 5.4. Last part of pre – processing were made in ArcGIS 10.5.

5.2.1.1 Radiometric calibration

Conversion of digital numbers to top of atmosphere (TOA) radiance was made in ENVI 5.4 by tool named *Radiometric calibration* using the following method:

$$L_{\lambda} = M_L * Q_{CAL} + A_L \quad (2)$$

L_{λ} = TOA spectral radiance (Watts/(m² * srad * μm)), M_L = Band-specific multiplicative rescaling factor from the metadata (RADIANCE_MULT_BAND_x, where x is the band number) A_L = Band-specific additive rescaling factor from the metadata (RADIANCE_ADD_BAND_x, where x is the band number) Q_{CAL} = Quantized and calibrated standard product pixel values (DN) (U.S. Geological Survey).

5.2.1.2 Cloud mask

Multispectral image from 2016 contains small area of cloud cover which has to be masked due to usage of quick atmospheric correction (QUAC), which is highly sensitive on presence of clouds on image. For masking was used software ENVI 5.4, where author manually localized cloud coverage by tool region of interest (ROI) and after masked this shapefile out of raster by giving cloud pixels *NoData* value.

5.2.1.3 Atmospheric correction

For both multispectral images was used QUAC atmospheric correction in ENVI 5.4.

QUAC determines atmospheric correction parameters directly from used raster's pixels, without ancillary information. QUAC is more approximate than FLAASH or other physics- based methods and also it is much faster because it does not involve first principles RT calculations. QUAC is based on empirical assumption that the reflectance of different materials (except highly structured materials: vegetation, shallow water and mud) is not dependent on particular scene (Bernstein, 2012).

“ENVI uses the latest QUAC algorithm described in Bernstein et al. (2012). This implementation contains the following enhancements to improve the accuracy of atmospheric correction:

- *Applies mud filtering to exclude highly structured materials,*
- *selects endmembers based on a small subset of available bands for most sensors. When a sensor spans both the visible and NIR-SWIR spectral regions, the algorithm excludes bands in the visible region,*
- *constrains the gain curve to be constant for wavelengths below 650 nm,*
- *suppresses the effects of dense vegetation,*
- *removes cloud endmembers for hyperspectral sensors with 940 to 1020 nm water absorption bands.” (Harris Geospatial).*

5.2.1.4 Normalized difference vegetation index

Normalized difference vegetation index (NDVI) is broadly used tool which quantifies vegetation by measuring difference between near- infrared (which vegetation strongly reflects) and red light (which vegetation absorbs). It always ranges from -1 to +1, when, if is it negative value there is highly likely absence of vegetation and closer to positive maximum is high possibility of dense vegetation(GIS Geography).

NDVI uses NIR and Red channel in its formula:

$$NDVI = \frac{(NIR-Red)}{(NIR+Red)} \quad (3)$$

Healthy vegetation reflects more NIR and green light compared to other wavelengths. But it absorbs more red and blue light and that’s why we see vegetation as a green colour (GIS Geography).

In Figure 12, the spectral curve of unhealthy vegetation shows that there is very less absorption of sunlight or more reflectance in red band (620 – 750 nm) rather in case of healthy vegetation. In near-infrared band ((750 to 1400 nm)) the reflectance is also very low as maximum of energy is being absorbed in NIR band (GIS Resources).

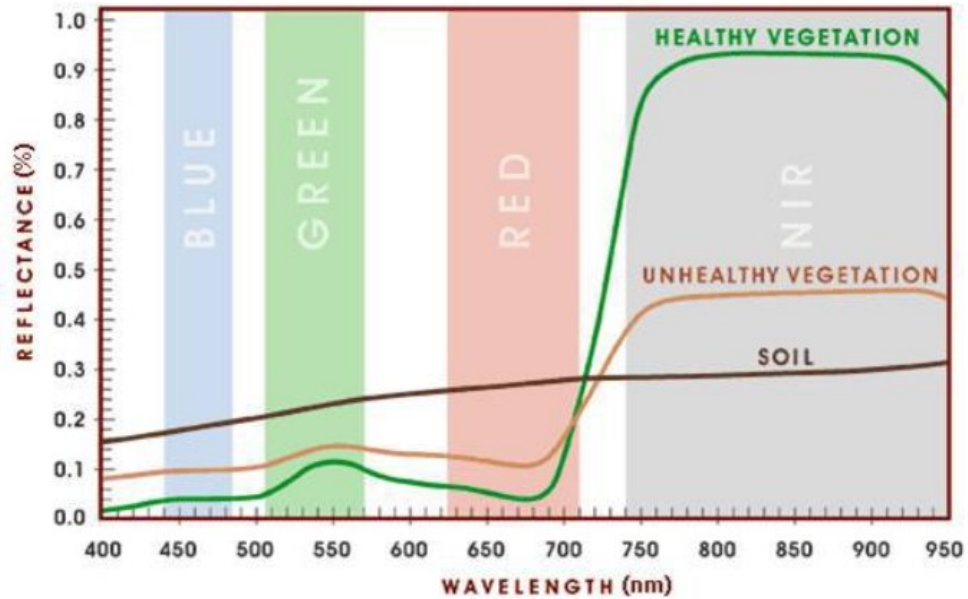


Figure 12: Spectral Curve of Healthy and Unhealthy vegetation (GIS Resources).

5.2.1.5 Normalized difference build-up index

Built-up surface have higher reflectance in SWIR wavelength range than in NIR wavelength range.

$$NDBI = \frac{(SWIR - NIR)}{(SWIR + NIR)} \quad (4)$$

5.2.1.6 Normalized difference water index

The NDWI index is most appropriate tool for water body mapping. The water bodies have strong absorbability and low radiation in the range from visible to infrared wavelengths.

The index uses the GREEN and NIR bands of RS images based on this phenomenon. The NDWI can enhance the water information effectively in most cases. It is sensitive to built-up land and often results in over-estimated water bodies (Sentinel-Hub) Water bodies have value $NDWI \geq 0.2$, smaller value contains even moisture in soil.

$$NDWI = \frac{(GREEN - NIR)}{(GREEN + NIR)} \quad (5)$$

5.2.1.7 Built-up index

Built-up index (BI) is the binary image with only higher positive value indicates the built-up and barren thus, allows BI to map the built-up area automatically. Thanks to different spectral profiles of components is possible to separate them. For its higher relevance was BI used instead of Normalized difference composite index.

Following description of extraction IS was made according Son (2016). Urban area for RS purposes can be described as a composition of IS, vegetation and exposed soils, while ignoring water. Thanks to different spectral profiles of components it is possible to separate them. For masking out, permanent water bodies is possible to use NDWI, if its value is greater than 0.2. It's impossible to use down to 0 values of NDWI because water is important component of soils and plants, the moisture has also effect on spectral properties of satellite data. Thus, these three indexes, NDBI, NDVI and NDWI are used for developing BI by following equation:

$$BI = NDBI - NDVI - (NDWI \geq 0.2) \quad (6)$$

Described process of extraction is the best known method to identify build-up areas in thesis study area. Son (2016) worked with data from Landsat OLI as author, for Landsat ETM data will same process applied. Because presence of bare soil in BI, it is not suitable for conclusive comparison between the years 2002-2016 in this thesis, but it is key input for extraction of IS for year 2016.

5.2.2 Thermal images pre-processing

All steps of thermal images pre – processing were made in ENVI 5.4. and ArcGIS 10.5.

5.2.2.1 Radiometric calibration

For thermal images was used the same tool as for multispectral images already described in chapter 3.3.1.1 *Radiometric calibration*.

5.2.2.2 Thermal atmospheric correction

Atmospheric correction of thermal image from 2002 was made ENVI 5.4 by tool name *Thermal atmospheric correction*. This process approximated and removed the atmospheric contributions from thermal radiance data.

Harris Geospatial describes this process as following: “*The algorithm first determines the wavelength that most often exhibits the maximum brightness temperature. This wavelength is then used as the reference wavelength. Only spectra that have their brightest temperature at this wavelength are used to calculate the atmospheric compensation. At this point, for each wavelength, the reference blackbody radiance values are plotted against the measured radiances. A line is fitted to the highest points in these plotted data and the fit is weighted to assign more weight to regions with denser sampling. The compensation for this band is then applied as the slope and offset derived from the linear regression of these data with their computed blackbody radiances at the reference wavelength.*

Upwelling atmospheric radiance and atmospheric transmission are approximated using the following method. First, the surface temperature of every pixel is estimated from the data and used to approximate the brightness temperature using the Planck function and assuming an emissivity of 1. Next, a line is fitted (using one of two methods) to a scatter plot of radiance vs. brightness temperature. The atmospheric upwelling and transmission are then derived from the slope and offset of this line.”

Atmospheric correction of thermal image from 2016 was made in ArcGIS 1.5 because image is acquired by Landsat 8 (TIRS), which is using two thermal bands (Band 10 and 11) and band 11 is currently not recommended for usage (U.S. Geological Survey, Atm Corr). Following equation is proposed as a suitable solution:

$$L_{TOA} = \tau \varepsilon L_T + L_u + \tau(1 - \varepsilon)L_d \quad (7)$$

where τ = atmospheric transmission; ε is the emissivity of the surface, specific to the target type; L_T = radiance of a blackbody target of kinetic temperature T ; L_u = upwelling or atmospheric path radiance; L_d = downwelling or sky radiance; and L_{TOA} = the space-reaching or TOA radiance measured by the instrument. Radiances are in units of $W/m^2 \cdot sr \cdot \mu m$ and the transmission and emissivity are unitless (Barsi, 2005).

5.2.2.3 Conversion of radiation to temperature

Radiance to temperature conversions was made using the Planck equation or the Landsat specific estimate of the Planck curve:

$$T = \frac{k_2}{\ln\left(\frac{k_1}{L_\lambda} + 1\right)} - 273.15 \quad (8)$$

where T is the temperature in Kelvin; L_λ is spectral radiance in $W/m^2 \cdot sr \cdot \mu m$; and k_1 and k_2 are calibration constants given in metadata file of image, outcome is already converted to $^\circ C$ (Barsi, 2005).

5.2.2.4 Land surface emissivity

$$P_v = \left(NDVI - \frac{NDVI_{min}}{NDVI_{max}} - NDVI_{min}\right)^2 \quad (9)$$

where P_v = proportion of vegetation; NDVI = Normalized difference vegetation index; $NDVI_{min}$ = minimum value of used NDVI; $NDVI_{max}$ = maximum value of used NDVI; index is unitless as outcome.

$$\varepsilon = 0.004P_v + 0.986 \quad (10)$$

where ε is the emissivity of the surface; P_v = proportion of vegetation (Bahuri, 2015).

5.2.2.5 Land surface temperature

LST was calculated from At-Satellite Brightness Temperature T as (Weng, et al. 2004):

$$LST = \frac{T}{1 + \left(\frac{\lambda T}{c_2}\right) \ln(\varepsilon)} \quad (11)$$

Where λ = wavelength of emitted radiance; $c_2 = hc/s = 1.4388 \cdot 10^{-2} m \cdot K$; h = Planck's constant = $6.626 \cdot 10^{-34} J \cdot s$; s = Boltzmann constant = $1.38 \cdot 10^{-23} J/K$; c = velocity of light = $2.998 \cdot 10^8 m/s$

5.2.2.6 Urban thermal field variance index

Urban thermal field variance index (UTFVI) is quantitatively representation of UHI related with its impact on surrounding environment. UTFVI is based on LST

of specific area and intensity of UHI. The higher value of LST, higher is the UHI effect.

UTFVI is calculated using the following equation:

$$UTFVI = \frac{(T_s - T_{mean})}{T_{mean}} \quad (12)$$

Where T_s = LST of certain point (in Kelvin) and T_{mean} = Mean LST of the whole study area (in Kelvin) (Zhang, 2016). UTFVI was classified into six classes according Table 8, which is representation of different levels of UHI impacts.

Table 8: Thresholds of ecological evaluation index (Zhang, 2006).

Urban thermal field variance index	Urban heat island phenomenon	Ecological evaluation index
<0	None	Excellent
0.0005–0.005	Weak	Good
0.005–0.010	Middle	Normal
0.015–0.015	Strong	Bad
0.015–0.020	Stronger	Worse
>0.020	Strongest	Worst

5.3 Processing of images and data

All processing of images and data in this part of thesis were made in ArcGIS 1.5 and Microsoft Excel as Figure 13 shows. For possibility of further process was necessary some images convert from raster format to shapefile format.

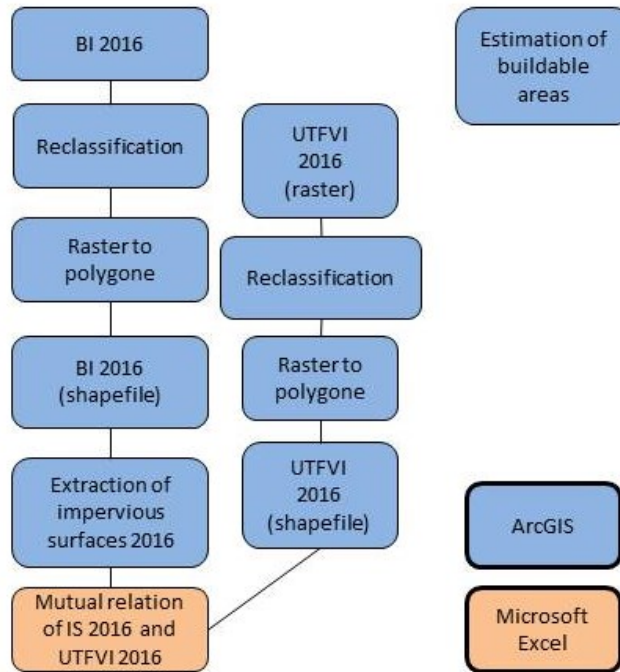


Figure 13: Workflow processing of images and data (Author).

5.3.1 Extraction of impervious surfaces 2016

BI is covering most of IS but it also includes bare soil and areas with lower level of vegetation. For determining of exact overview of IS was necessary to transform BI to shapefile and after erase arable land which author obtained from current land use of Prague. Unfortunately this data are available just for year 2016 and not for 2002, because of that extraction of IS was made just for year 2016. Outcome were intersected with current build-up area containing green surfaces which lead to exclusion of all bare soil from IS shapefile for higher precision of extraction. This process could be described as following:

$$IS = BI - LU_{AL} - BA_v \quad (13)$$

where IS = Impervious surfaces; BI = Build-up index; LU_{AL} = Arable land; BA_v = Build-up area containing vegetation from MP.

5.3.2 Estimation of future development areas

Future development of Prague is hard to predict, because of ongoing process of proposing Metropolitan plan. For author's prediction it is possible to use existing MP, which contains area which is possible to build on and also areas which are already build-up. That way author is able to obtain areas in Prague, where is possible to build but still there are no structures. Other important input is part of MP so called "Large development areas", which author combined with previous data and got outcome which covers most of area in Prague where the future development will be allowed. For better verifiability of result is BI without bare soil erased from future development layer because of strong relation of existence of UHI and IS.

$$FD = BU_{able} + LDA - BA - BI - LU_{AL} \quad (14)$$

where FD = Future development; BU_{able} = Build able area, LDA = Large development area; BA = Build-up area; BI = Build-up index; LU_{AL} = Arable land.

5.3.3 Mutual relation of IS and UHI

For prediction it is necessary to create quantitative estimation how much IS is affecting UHI intensity. Extracted IS was used for clipping the shapefile of UTFVI 2016 and by this process author obtained area where is IS and intensity of UHI. From this mutual relation we can estimate how much, might future development affect local intensity of UHI.

5.4 Analogy and prediction

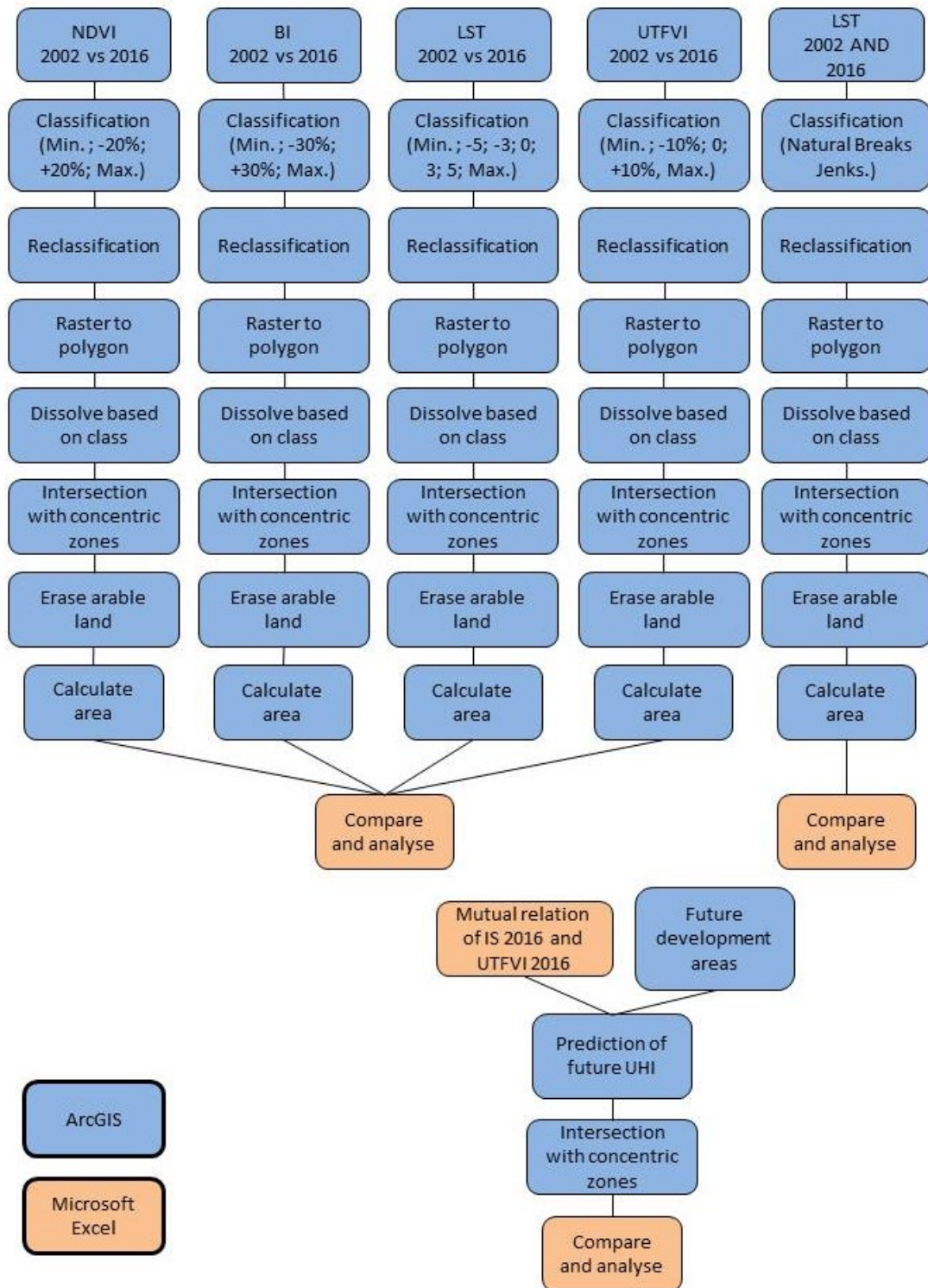


Figure 14: Workflow of analogy and prediction (Author).

In first part author compared and analysed all changes of studied features between years 2002-2016 and focused for patterns and relations. In second part

author retrieved relation between IS 2016 and UHI 2016 and based on the relation was able to predict future increase of area which UHI will cover as Figure 14 shows..

5.4.1 Analogy between 2002-2016

Four main outcomes and population growth were compared for better understanding how the city developed and UHI developed in selected time period. For increasing level of comparability author erased arable land from all compared features. Study area was divided on concentric zones based on Sýkora (2012) Figure 10. These four essentially different regions of Prague witness own specific urban development so analogy of all outcomes will be divided based on concentric zones of Prague.

5.4.1.1 NDVI

Comparison of NDVIs was dubious because of various reasons. Firstly, these indexes were obtained by different sensors which both have slightly different aspects. According to Ke (2015), in similar conditions solar geometry and meteorological visibility, i.e., the same level of aerosols, Landsat 8 OLI produces slightly higher TOA NDVI for trees and lower NDVI for water than Landsat 7 ETM+. Second and bigger challenge is a fact that every year provides different time of vegetation period, so amount of greenery is relative for comparison. Based on these facts author used 20% threshold values, without 0% value, for increasing the level of comparability.

5.4.1.2 BI

Most relevant analogy for build-up area would be comparison of IS between years 2002-2016. Author was unable to acquire IS 2002 due to lack of data. BI contain most of IS, but also bare soil and agricultural land which could misinterpret final results. Most of agricultural land was erased in a form of arable land, but bare soil might still occurred. Based on these facts author used 30% threshold values, without 0% value, for increasing the level of comparability.

5.4.1.3 UTFVI

Quantitative representation of the intensity of UHI and its impact on the environment is UTFVI key factor of comparison. As threshold values were selected

10% and 0% which clearly shows focal areas of escalation or contraction between years. As a threshold values were selected 10% and 0%. 10% is a equivalent of two UTFVI levels in Table 8.

5.4.1.4 LST

Analogy of LST was included as controlling indicator of rapid temperature changes in area and provides, unlike the UTFVI, specific temperature data. Combination of UTFVI and LST provides clear concept of UHI growth, impacts and specific computable temperatures. As a threshold values were selected 5 °C, 3 °C and 0 °C. For better understanding also quantitative representation of LST was elaborated. For classification of LST 2002 and 2016 was used. Natural Breaks (Jenks) method with 8 classes, which created intervals based on the inputs volume.

5.4.2 Prediction based on MP

Prognosis of future growth of UHI in Prague is focused on increase of area which UHI will cover in near future. There were two main inputs for this process. First was estimated future development area based on current MP of Prague and future development zones. Secondly was used mutual relation of IS 2016 and UTFVI 2016, which represents the degree of influence how much IS is quantitatively related to UHI. Final outcome is in variant of highest possible intensity of UHI in future developed areas assuming the highest possible intensity of building.

6 RESULTS

Several factors in each urban zone (Appendix 3) have been compared and evaluated in an effort to identify the impact of urban development on UHI. All studied phenomena were intertwined and significantly influenced each other. Outputs have been described in two basic planes. The first plane was a numerical interpretation in percentages, which was a quantitative representation of the change. The second plane was visible from the map outputs, which showed the spatial expression of data and allowed to monitor their spatial distribution.

Mutual relation of IS and UTFVI (Appendix 8) was unequivocal. IS with a source of thermal radiation were main factors causing UHI and more than 80% of IS in Prague in 2016 actually were in the highest level of UTFVI. There was also 10,38% of IS which intersected with the lowest level of UTFVI, which was caused by the edges of water bodies mainly river Vltava. Secondary effect is caused by the areas with dense vegetation and also settlements outside of Prague's build-up main area, which had lower intensity and higher intensity of vegetation.

6.1 Downtown

Appendix 1 showed the only zone of the city recorded a population decline (4.56%), which moved to other zones of Prague or outside Prague is downtown. This fact, however, was not so important to assess for the study of UHI change in the downtown, as people had moved away but urban structures stayed. This was evident in the BI change, where the downtown has not made any major changes. A surprising change was evident in the NDVI, where there was a green area growth in the downtown. The author attributed this sudden green wave to the different beginnings of the vegetation season in both studied years, and of course this factor had a significant impact on the development of the city's temperatures. The intensity of the UHI had a decreasing trend in the downtown due to a higher intensity of vegetation. Different local climatic conditions have also played a role, which have not been elaborated in respect of the scope of work. It was apparent from the Appendix 2 what temperature drop occurred at more precise temperature intervals. Higher interval 32.66 - 34.95 °C crashed into lower intervals. This suggests that this was not a sudden and intense change in trend, but only a reduction in the share of plots in

maximum values up to several orders of magnitude below. The prediction (Appendix 9) attributed a 0.00% increase in the area of the highest UHI intensity, which was due to the absence of the area for the new development.

6.2 Inner city

The inner city recorded the lowest income of 5.31%, who had a permanent address in this zone of Prague (Appendix 1). This factor was to a lesser extent already reflected in a slight increase in the new building, which was evidenced by a slight increase in BI intensity. The NDVI was slightly higher as expected (Appendix 1; 4). Surface temperature increased slightly in this zone, and in the Appendix 2 was evident that the increase in the mean values was due to the decrease of the areas with lower temperatures but also to the decrease of the areas of higher temperatures. This could be caused by more intensive vegetation and a new development in this zone. The UHI intensity was slightly lower, but a slight increase in the highest interval was also evident (Appendix 1; 6; 7). Prediction (Appendix 9) attributed to an inner city a 3.00% increase in area of the highest UHI intensity. This is a slight increase with negligible influence on the environment and urban microclimate.

6.3 Outer city

Outer City was the second largest recipient of the new population just behind Outskirt. Almost the same amount but different percentage growth. The 12.74% increase in the population was already more pronounced in the new construction, showing an increase of the third category BI by 4.62% (Appendix 1). The NDVI was slightly higher as expected (Appendix 1; 4). The surface temperature also increased significantly by more than 3 °C. Appendix 2 showed the same trend as in the inner city, where the rise in mean intervals was due to the decrease in areas with lower temperatures but also to the decrease in the areas of higher temperatures. This could be caused by more intensive vegetation and a new development in this zone. UHI intensity increased in the fourth UTFVI category by 3.29%, which in the context of this zone can be considered a moderate increase (Appendix 1; 6; 7). Prediction (Appendix 9) of outer city attributed 9.70% increase in the UHI highest intensity area. This was a marked increase with an obvious impact on the environment and urban microclimate.

6.4 Outskirt

Appendix 1 showed that outskirts had the highest population growth in all Prague zones. Between 2002 and 2016, there was an increase of 45.52% of the population, which led to the construction of areas in this zone. Third BI category grew by 5.45%, which was the highest measured value of all Prague zones (Appendix 1; 4). In proportion to the number of new inhabitants there was not such a significant change. The role could also play a type of buildings that could be less identifiable, for example, a family house that is less recognizable in a 30-m pixel. The change in surface temperature at 2.16% was more than 5 ° C, due to the new development in the area (Appendix 1). In Appendix 2, it clearly showed the sudden drop in the minimum intervals and the increase in the mean intervals, indicating a higher amount of significant changes in surface use. The change in UHI intensity was significant and confirmed a higher degree of build-up than what the author was able to identify. 48.17% grew by less than 10% UTFVI and 5.24% increased by more than 10%, where 10% are approximately two degrees of ecological vulnerability index (Appendix 1; 6; 7). Prediction (Appendix 9) for outskirts attributed a 35.50% increase in the area of the highest UHI intensity. This was an extreme increase that will have significant impacts on the environment and urban microclimates. Most of these areas are currently greenery or agricultural land.

7 DISCUSSION

Migration in Prague area can be divided into two types. Some newcomers migrate from other parts of the country, that's the process called *urbanization*. Others migrate within Prague area and its surroundings and this can be understood as *suburbanization*. In the European context, the growth of Prague between 2002 and 2016 was 9.82% of the population, which is not anything extraordinary. In the global context, these are very low values in comparison with Africa or Asia (UN, 2014). Despite the fact that we do not experience any extreme migration of people in Prague, these relatively small changes can still have significant impacts on the environment and quality of life. Removal of greenery has a demonstrable effect on local climatic conditions (Gunawardena, 2017). The new build-up areas degrade the agricultural land because it removes the top most fertile soil layer and physically occupies area. This leads to a steady reduction in the amount of farmland.

The UHI in Prague is growing along with the number of inhabitants. The downtown has the smallest share of this change and gradually increasing build-up area of the other three studied zones considerably increases UHI intensity in Prague. Expansion of IS is the main reason for the growing UHI area. It is not possible, however, to look at this problem by taking account at how much less housing will be build, the less negative effects of UHI will be. The preferred approach should be to actively adapt urban structures and implement measures to reduce the temperatures in the urban environment. These measures exist and their effectiveness is demonstrated by a wide range of studies (Gunawarden, 2017; U.S. Environmental Protection Agency, 2012; Santamouris, 2013) and examples of long-term usage (Nymag). City of Prague has created a strategy for combating climate change. This strategy analyzes and looks for a solution to the growing intensity of a number of phenomena that negatively affect the functioning of the city and the lives of the population. There is also a growing UHI intensity included, so we can expect Prague to actively participate in reducing the vulnerability of the city (IPR Praha, 2016).

There are a number of studies investigating the intensity of UHI and its change over time. The most effective way of investigating surface UHI is RS (US Environmental Protection Agency, 2012; UHI Assayment Manual, 2014). A very common element in these studies is to investigate the effect of land use / land cover

change over a certain time horizon (Bokaie, 2016; Singh, 2016; Son, 2016). Interpretation of the UHI itself differs, some studies interpret only the UHI intensity in the form of temperature differences (Zhang, 2016), and other studies quantitatively express the intensity and impact on the environment using UTFVI (Singh, 2016). In this work, the author used a holistic approach, examining the entire interconnected system of phenomena and factors by measuring individual parts and subsequent interpretations as a whole. Therefore, he used the above-mentioned procedures to analyse the issue. The author used the distribution in the concentric zones (Ouředníček, 2012), where each zone has its specific spatial urban development. Thanks to this, the author had more references to what the changes meant and what their causes were. The data from Landsat 7 and Landsat 8 sensors in 30-meter pixel resolution has proven to be an appropriate precision for this type of analysis and the size of the studied area. Thanks to this resolution, these data can be used for future research in more accurate local detail and can be targeted at individual city districts or neighborhoods. Assess how a particular type of building, in combination with its specific climatic conditions, influences the temperature balance in a certain location.

The final outputs of the work showed a significant continuity of the UHI intensity increase in the locations where the new build-up areas occurred and the intensity of the vegetation decreased. This has been confirmed by a number of studies and could be called the current paradigm. However, the work was focused on the study of specific conditions of influence, which urban development in Prague has on UHI. It has been shown that a direct proportion cannot be applied between the number of people immigrated and the increase in UHI intensity. The main role is played by the type of urban structures, which is different in individual concentric zones and amount of IS. A follow-up study on this work could, for example, characterize the basic typology of buildings in individual urban areas and then assess their impact on local temperature conditions. The detailed dataset of MP allowed the author to predict the future extent of the UHI expansion in Prague. The increase in UHI is zero in the downtown and then rises gradually from the downtown of the city to the edges, where the largest amount of newly built-up areas are concentrated and more will be build.

8 CONCLUSION AND CONTRIBUTIONS

The outputs of the thesis confirmed paradigm of the IS relation with the presence of surface UHI. Comparison of people migration with UHI showed that UHI growth is not directly proportional to gain of people in area. Outer city and outskirts recorded the largest population growth, and yet the increase in UTFVI was not as significant as expected. All concentric zones recorded different trends over the period. Population growth rose from the downtown to the edges of the city, and the outskirts had the highest population growth of 45.52% between 2002 and 2016, but there was still no massive UTFVI growth in the area. The prediction shows the future development of the surface UHI in Prague, where the growth trend will be the same as it has been so far in the sense of spreading from the downtown with a low intensity to the edge with increasing intensity. The most dynamic regions were outer city and outskirts, which had the most significant change.

All of the work goals were met by the planned methodology, where the images at a resolution of 30 meters from the Landsat sensors proved to be the appropriate dataset to analyse this detail and study area dimensions. The first contribution of this work was the use of existing UHI assessment methods from other parts of the world in Prague, where there are not many studies on this topic. Second contribution was the appropriate combination of these research methods with the spatial planning documentation of Prague. This made it possible to modify and refine the used methodology and to predict future development of UHI on the basis of future urban development.

The results of the work showed differences in urban zones of Prague and their different impacts on UHI growth. The data from this thesis could be used for a study in more detail of individual urban parts of city, where it would be possible to work with knowledge of local climatic conditions and specific typology of buildings. The methodology of data interpretation might be also combined with local measurements which atmospheric UHIs could also be studied and how the surface UHI influences it and vice versa. The author has learned a lot about geoinformatic procedures, remote sensing and operations with ENVI and ArcGIS software, which was one of the reasons for this work. The interdisciplinarity contained in a combination of different types of input data showed a high degree of variety of possible ArcGIS operations.

9 REFERENCES

9.1 Literature sources

BARSI J.A. et al. (2005): Validation of a Web-Based Atmospheric Correction Tool for Single Thermal Band Instruments. Proceedings of SPIE, Vol. 5882.

BERG et al. (1982): A Study of Growth and Decline. Urban Europe, 1. Pergamon Press. Oxford. ISBN: 978-0-08-023156-3

BERNSTEIN L. et al. (2012): Quick atmospheric correction code: Algorithm description and recent upgrades. Optical Engineering November 2012.

BOKAIE M. (2016): Assessment of Urban Heat Island based on the relationship between land surface temperature and Land Use/ Land Cover in Tehran. Sustainable Cities and Society 23 (2016), p. 94–104.

BUYANTUYEV A. et al. (2010): Urban heat islands and landscape heterogeneity: linking spatiotemporal variations in surface temperatures to land-cover and socioeconomic patterns. Landsc. Ecol. 25, p. 17–33.

OULOS L. et al. (2003): Passive cooling of outdoor urban spaces. The role of materials. Solar Energy 77, p. 231-249.

GAGO E. J. et al. (2013): The city and urban heat islands: A review of strategies to mitigate adverse effects. Renewable and Sustainable Energy Reviews 25 (2013), p. 749-758

GUNAWARDENA K. R. et al. (2017): Utilising green and bluespace to mitigate urban heat island intensity. Science of the Total Environment 584-585, p. 1040-1055.

IMHOFF M. L. et al. (2010): Remote sensing of the urban heat island effect across biomes in the continental USA. Remote Sens. Environ. 114, p. 504–513.

KE Y. et al. (2015): Characteristics of Landsat 8 OLI-derived NDVI by comparison with multiple satellite sensors and in-situ observations. Remote Sensing of Environment 164 (2015) p. 298–313

KLEEREKOPER I. et al. (2012): How to make a city climate-proof, addressing the urban heat island effect. Resources, Conservation and Recycling 64, 30-38.

- LARIVIERE I. et al.** (1999): Modelling the electricity consumption of cities: effect of urban density. *Energy Economics* 21, p. 53-66.
- MAIER K. et al.** (2012): Udržitelný rozvoj území. Grada Publishing, a.s. Prague. ISBN: 978-80-247-4198-7
- MWANIKI M. W. et al.** (2015): A comparison of Landsat 8 (OLI) and Landsat 7 (ETM+) in mapping geology and visualizing lineaments: A case study of central region Kenya. 36th International Symposium on Remote Sensing of Environment, 11–15 May 2015, Berlin, Germany.
- OUŘEDNÍČEK M.** (2000): Theory of Stages of Urban Development and Differential Urbanisation. *Geografie. Sborník ČGS*, 105, 4, p. 361-369
- OUŘEDNÍČEK M. et al.** (2012): Sociální proměny pražských čtvrtí. Published by Academia 2012, 302 pages. Prague. ISBN: 978-80-200-2064-2
- PRAKASH A.** (2000): Thermal remote sensing: concepts, issues and applications. *International Archives of Photogrammetry and Remote Sensing*. Vol. XXXIII, Part B1. Amsterdam.
- PŮR ČR** (2015): Politika územního rozvoje České republiky, ve znění Aktualizace č.1, Ministerstvo pro místní rozvoj.
- RIZWAN A. M. et al.** (2008): A review on the generation, determination and mitigation of Urban Heat Island. *Journal of Environmental Sciences* 20, 120-128.
- SANTAMOURIS M.** (2012): Using cool pavements as a mitigation strategy to fight urban heat island—A review of the actual developments. *Renewable and Sustainable Energy Reviews* 26 (2013) p. 224–240
- SANTOS A. R.** (2017): Spatial and temporal distribution of urban heat islands. *Science of the Total Environment* 605-606, p. 946-956.
- SINGH P. et al.** (2016): Impact of land use change and urbanization on urban heat island in Lucknow city, Central India. A remote sensing based estimate. *Sustainable Cities and Society* 32, p. 100-114.
- SON N. et al.** (2016): Assessment of urbanization and urban heat islands in Ho Chi Minh City, Vietnam using Landsat data. *Sustainable Cities and Society* 30, p. 150-161.

SÝKORA L. et al. (2012): Prague: Urban Growth and Regional Sprawl. Confronting Suburbanization : Urban Decentralization in Postcosialist Central and Eastern Europe, First Edition. Published 2014 by John Wiley, Ltd., ISBN: 978-1-405-18548-6

TAHA H. (1975): Modelling the impacts of large-scale albedo changes on ozone air quality in the south coast air basin. Atmospheric Environment Vol. 31, No. 11, p. 1667-1676.

ÚAP HL. M. PRAHY (2008): Územní analytické podklady Hlavního města Prahy. Institut plánování a rozvoje hl. m. Prahy.

HOVE L. W. A. (2011): Exploring of Urban Heat Island Intensity of Dutch cities. Alterra report 2170, Wageningen.

VOOGT J. A. et al. (2002) Thermal remote sensing of urban climates. Remote sensing Environment 86, p. 370- 384.

WENG Q. et al. (2003): Estimation of land surface temperature–vegetation abundance relationship for urban heat island studies. Remote Sensing of Environment 89 (2004), p. 467–483.

ZÁKON Č. 225/2017 Sb, NOVELA STAVEBNÍHO ZÁKONA. Ministerstvo pro místní rozvoj ČR.

ZEMEK F. (2013): Aerial remote sensing. Centrum výzkumu globální změny AV Č. Brno. Czech Republic. ISBN: 978-80-87902-05-9

ZHANG Y. et al. (2006): Land surface temperature retrieval from CBERS-02 IRMSS thermal infrared data and its applications in quantitative analysis of urban heat island effect. Journal of Remote Sensing Volume 10, Issue 5, Pages 789-797.

9.2 Internet sources

ATM CORR. (online) Available at: <https://atmcorr.gsfc.nasa.gov/>
(Accessed 14th of December 2017)

BAHURI U. (2015): Landsat 8: Estimating Land Surface Temperature Using ArcGIS. (online). Available at:
<https://www.youtube.com/watch?v=uDQo2a5e7dM>
(Accessed 10th of February 2018)

ČHMÚ and IPR. (2013). (online). Available at:
http://www.iprpraha.cz/uploads/assets/soubory/data/projekty/UHI/Co_vime_o_tepelnem_ostrovu_Prahy.pdf

(Accessed 10th of February 2018)

GIS GEOGRAPHY. (online) Available at: <https://gisgeography.com/ndvi-normalized-difference-vegetation-index/>.

(Accessed 2nd of January 2018)

GIS RESOURCES. (online) Available at: <http://www.gisresources.com/ndvi-ndbi-ndwi-ranges-1-1/>

(Accessed 18th of December 2017)

HARRIS GEOSPATIAL. (online) Available at:
<http://www.harrisgeospatial.com/docs/backgroundquac.html>

(Accessed 8th of January 2017)

IPR PRAHA. (online) Available at:
<http://www.iprpraha.cz/clanek/58/prostorova-regulace>

(Accessed 10th of November 2017)

IPR (2016): Strategie adaptace hl. m. Prahy na klimatickou změnu. (online)
Available at:

http://www.iprpraha.cz/uploads/assets/dokumenty/ssp/Adaptacni%20strategie/IPRPraha_Adaptacni_strategie_analyticka_cast_FINAL.pdf

(Accessed 5th of March 2018)

METEO BLUE. (online) Available at:
https://www.meteoblue.com/en/weather/forecast/multimodel/prague_czech-republic_3067696

(Accessed 18th of February 2018)

NATURAL RESOURCES CANADA. (online) Available at:
<http://www.nrcan.gc.ca/node/14623>

(Accessed 15th of December 2017)

NYMAG. (online) Available at:
<http://nymag.com/daily/intelligencer/2016/06/how-cities-are-combating-rising-temperatures.html>

(Accessed 19th of February 2018)

OPTICS FOR HIRE. (online) Available at:
<http://www.opticsforhire.com/blog/2015/7/15/design-of-ir-lenses>

(Accessed 15th of December 2017)

SENTINEL-HUB. (online) Available at: <https://www.sentinel-hub.com/eoproducts/ndwi-normalized-difference-water-index>

(Accessed 3rd of December 2017)

UHI ASSESMENT MANUAL (2014):. (online). Available at: http://eu-uhi.eu/download/publications/wp4/WP4.2_UHI_Assessment_Manual.pdf

(Accessed 10th of February 2018)

UN (2014): World Urbanization Prospects: Highlights. 2014 Revision. United Nations, New York. (online) Available at:
<https://esa.un.org/unpd/wup/publications/files/wup2014-highlights.pdf>

(Accessed 5th of January 2018)

U.S. ENVIRONMENTAL PROTECTION AGENCY (2012): Reducing Urban Heat Islands: Compendium of Strategies (online) Available at:
<https://www.epa.gov/heat-islands/heat-island-compendium>

(Accessed 3rd of December 2017)

U.S. GEOLOGICAL SURVEY. (online) Available at:
<https://landsat.usgs.gov/how-do-landsat-8-band-combinations-differ-landsat-7-or-landsat-5-satellite-data> and <https://landsat.usgs.gov/using-usgs-landsat-8-product>

(Accessed 22nd of November 2018)

VOOGT J. A. (2004): Urban Heat Islands: Hotter Cities. (online) Available at:
<http://www.actionbioscience.org/environment/voogt.html>

(Accessed 5th of January 2018)

10 LIST OF FIGURES

Figure 1: Metropolitan Development Model (Berg 1982).....	4
Figure 2: Causes of UHI (Kleerekoper, 2012).....	8
Figure 3: Evapotranspiration and Shading on a Green Roof (U.S. Environmental Protection Agency, 2012).....	11
Figure 4: Intensity of Prague’s UHI (ČHMÚ and IPR, 2013).....	14
Figure 5: Change of average daily T_{\min} between 2001-2001 and 1961-1970 (ČHMÚ and IPR, 2013)	14
Figure 6: Infrared portion of the electromagnetic spectrum (Optics for hire).	16
Figure 7: Bandpass wavelengths for Landsat 8 OLI and TIRS sensor, compared to Landsat 7 ETM+ sensor (U.S. Geological Survey).	18
Figure 8: Geographical map of the Capital city of Prague (ČÚZK).....	20
Figure 9: Average precipitation total in Prague (Meteo Blue).....	21
Figure 10: Division into concentric zones (Author, based on Ouředníček, 2012)....	22
Figure 11: Workflow pre-processing of images and data (Author).....	27
Figure 12: Spectral Curve of Healthy and Unhealthy vegetation (GIS Resources)..	30
Figure 13: Workflow processing of images and data (Author).	35
Figure 14: Workflow of analogy and prediction (Author).....	37

11 LIST OF TABLES

Table 1: Basic Characteristics of Surface and Atmospheric UHIs (U.S. Environmental Protection Agency, 2012).....	7
Table 2: Landsat Enhanced Thematic Mapper Plus (ETM+) (U.S. Geological Survey).....	17
Table 3: Landsat 8 Operational Land Imager (OLI) and Thermal Infrared Sensor (TIRS) (U.S. Geological Survey).....	17
Table 4: Population in Prague 1991 - 2016 (Author, based on Czech Statistical Office).....	24
Table 5: Change of population 1991 - 2016 (Author, based on ČSÚ).....	24
Table 6: Used data (Author).....	25
Table 7: Overview of meteorological conditions of selected time periods (Author).26	
Table 8: Threshold of ecological evaluation index (Zhang, 2006).	34

12 LIST OF APPENDIX

Appendix 1: Comparisons between 2002 and 2016 (Author).....	55
Appendix 2: Comparison of LST between 2002 and 2016 (Author).....	56
Appendix 3: Concentric zones of Prague (Author).....	57
Appendix 4: NDVI and BI differences between 2002 and 2016 (Author).....	58
Appendix 5: LST 2002, 2016 (Author).....	59
Appendix 6: UTFVI 2002, 2016 (Author).....	60
Appendix 7: LST and UTFVI differences (Author).....	61
Appendix 8: Relation of IS and UTFVI 2016 (Author).....	62
Appendix 9: Prediction of near future development (Author).....	63

13 APPENDIX

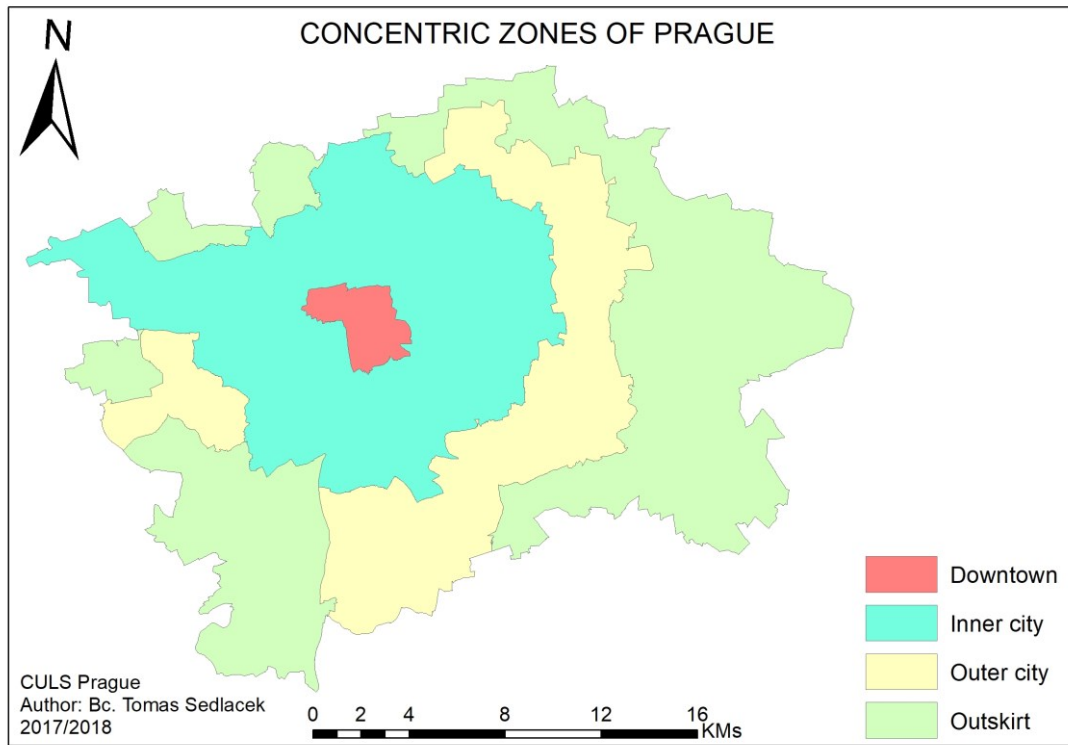
	Urban zones		Downtown	Inner city	Outer city	Outskirt	Prague area
	Population		-3 774	35 461	40 687	41 703	114 077
Change 2002 - 2016			-4,56%	5,31%	12,74%	45,52%	9,82%
	NDVI (Appendix 4)	Decreased more than 20%	0,04%	1,04%	2,45%	3,45%	2,15%
		Some change	94,00%	91,32%	90,33%	90,25%	90,80%
		Increased more than 20%	5,96%	7,64%	7,22%	6,29%	7,05%
	BI (Appendix 4)	Decreased more than 30%	0,06%	0,49%	0,57%	1,05%	0,68%
		Some change	99,76%	97,84%	94,81%	93,50%	95,72%
		Increased more than 30%	0,18%	1,68%	4,62%	5,45%	3,59%
	UTFVI (Appendix 7)	Decreased more than 10%	3,93%	5,00%	5,48%	3,65%	4,65%
		Decreased less than 10%	74,32%	60,49%	57,31%	42,94%	54,30%
		Increased less than 10%	21,67%	33,53%	33,92%	48,17%	38,14%
		Increased more than 10%	0,09%	0,98%	3,29%	5,24%	2,92%
	LST (Appendix 7)	Decreased more than 5 °C	0,00%	0,12%	0,29%	0,48%	0,27%
		Decreased 3-5 °C	0,06%	1,08%	1,39%	1,01%	1,11%
		Decreased less than 3 °C	58,74%	42,50%	39,12%	26,26%	36,75%
		Increased less than 3 °C	39,34%	54,01%	53,75%	65,04%	57,20%
		Increased 3-5°C	1,86%	2,10%	4,53%	5,05%	3,65%
		Increased more than 5°C	0,00%	0,19%	0,93%	2,16%	1,01%

Appendix 1: Comparisons between 2002 and 2016 (Author).

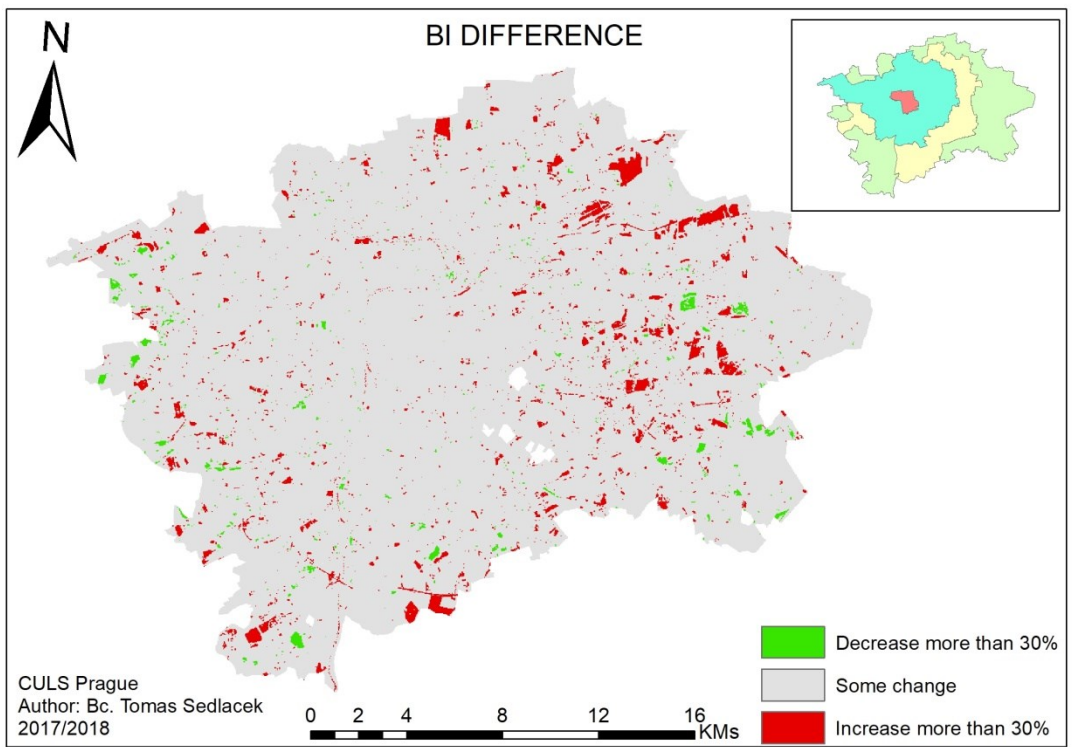
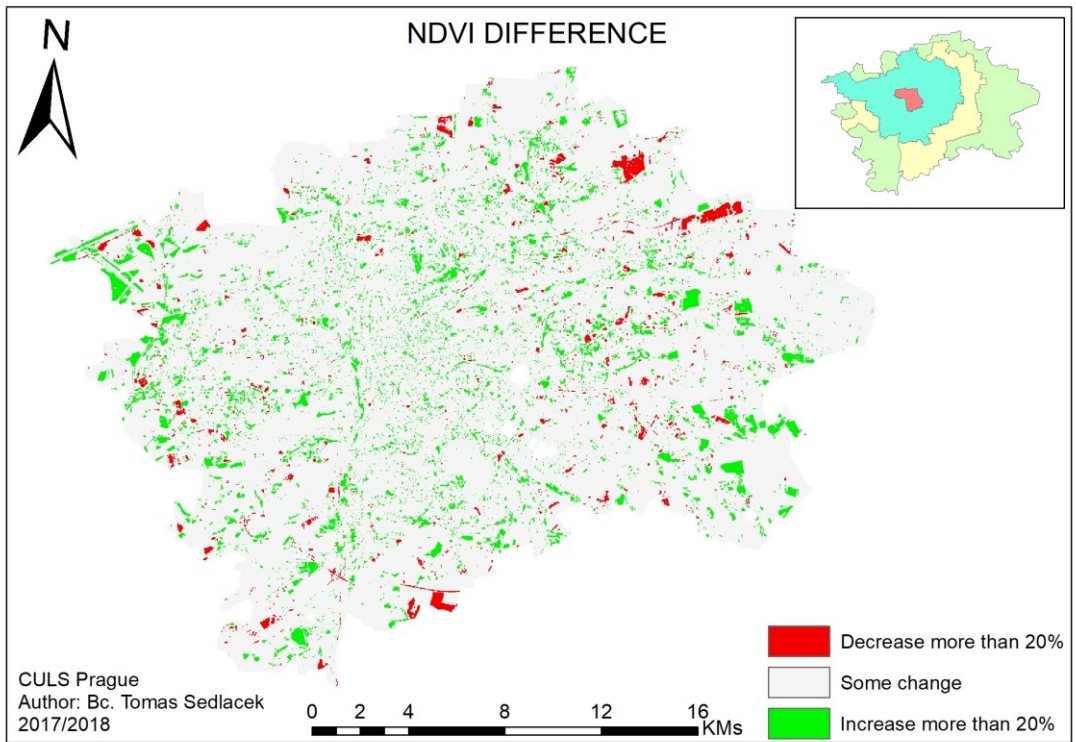
°C	LST									
	2002					2016				
	Downtown	Inner city	Outer city	Outskirt	Prague area	Downtown	Inner city	Outer city	Outskirt	Prague area
19.14 - 25.3	6,85%	5,43%	3,94%	14,21%	7,98%	5,02%	1,25%	0,42%	0,76%	0,98%
25.31 - 27.27	4,69%	13,52%	18,80%	29,67%	19,89%	4,31%	10,35%	13,95%	25,61%	16,09%
27.28 - 29.25	13,07%	17,80%	18,76%	23,96%	19,93%	10,78%	22,42%	21,32%	35,17%	26,05%
29.26 - 30.78	12,44%	21,36%	18,39%	16,39%	18,78%	22,14%	30,17%	27,02%	25,12%	27,54%
30.79 - 32.65	28,31%	27,52%	27,09%	11,58%	22,21%	46,25%	28,11%	29,63%	11,12%	23,35%
32.66 - 34.95	32,73%	12,18%	10,90%	3,45%	9,52%	10,68%	7,09%	6,72%	2,00%	5,42%
34.96 - 38.69	1,92%	2,03%	1,84%	0,63%	1,52%	0,81%	0,62%	0,92%	0,19%	0,56%
38.70 - 47.13	0,00%	0,16%	0,28%	0,11%	0,17%	0,00%	0,00%	0,02%	0,03%	0,02%

°C	Changes 2002-2016				
	Downtown	Inner city	Outer city	Outskirt	Prague area
19.14 - 25.3	-1,84%	-4,19%	-3,52%	-13,45%	-7,00%
25.31 - 27.27	-0,38%	-3,17%	-4,85%	-4,06%	-3,80%
27.28 - 29.25	-2,29%	4,62%	2,56%	11,21%	6,11%
29.26 - 30.78	9,71%	8,81%	8,63%	8,73%	8,76%
30.79 - 32.65	17,95%	0,59%	2,53%	-0,46%	1,15%
32.66 - 34.95	-22,05%	-5,09%	-4,18%	-1,45%	-4,10%
34.96 - 38.69	-1,10%	-1,42%	-0,92%	-0,44%	-0,97%
38.70 - 47.13	0,00%	-0,16%	-0,26%	-0,08%	-0,15%

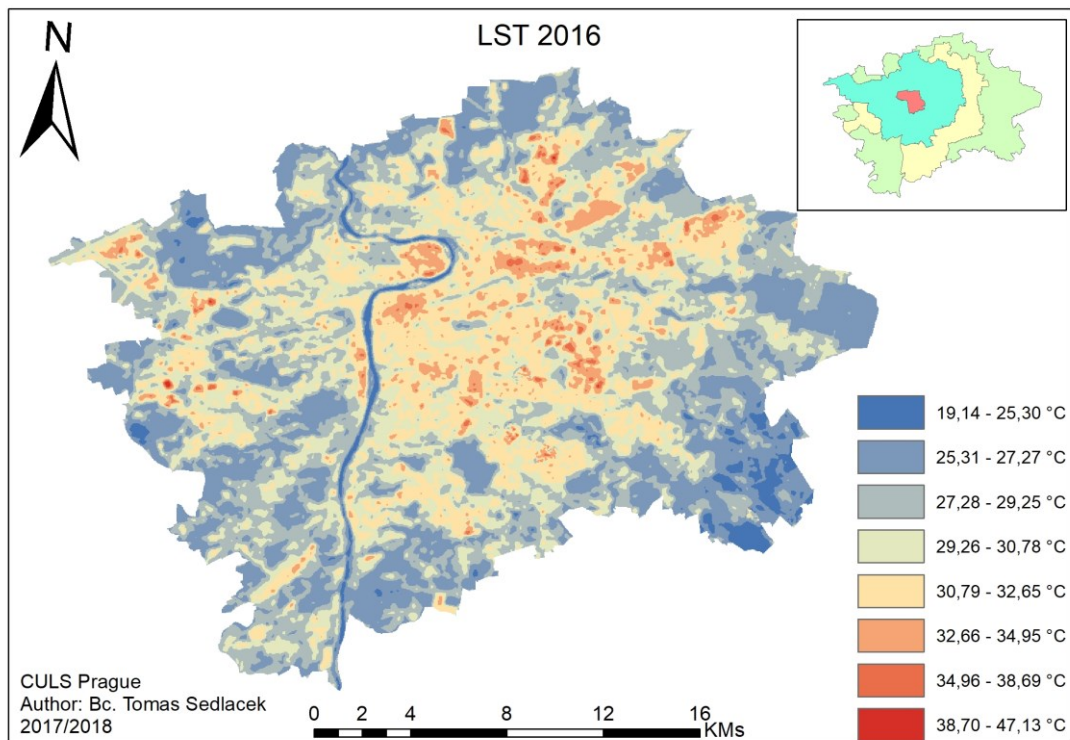
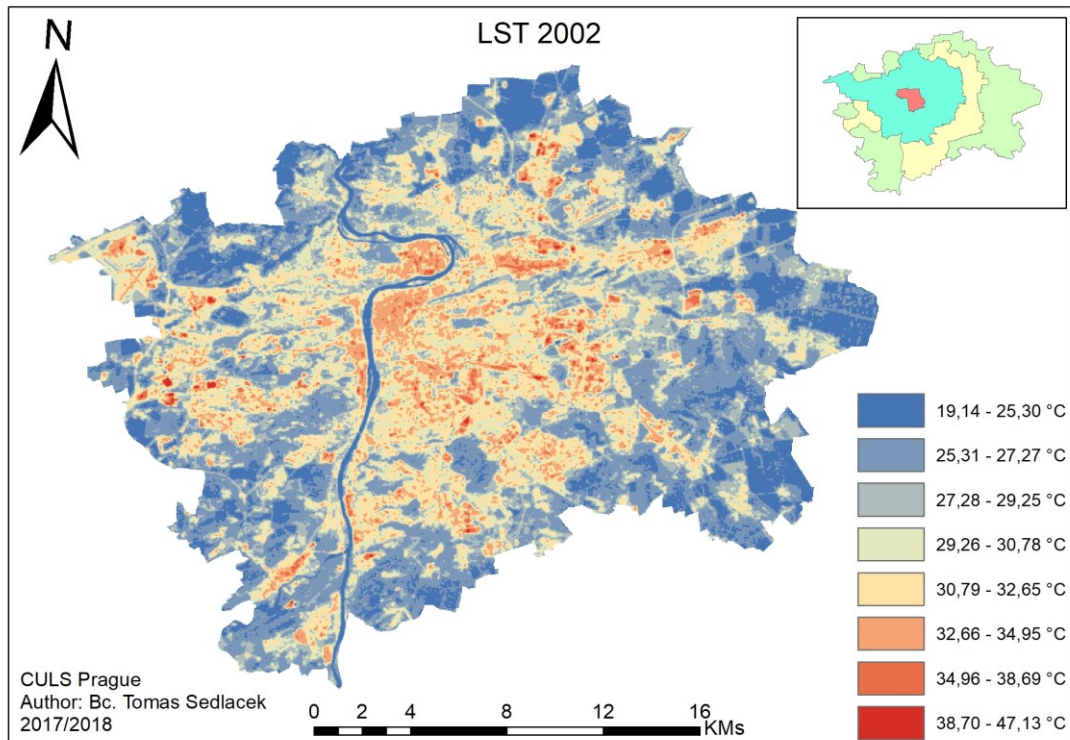
Appendix 2: Comparison of LST between 2002 and 2016 (Author).



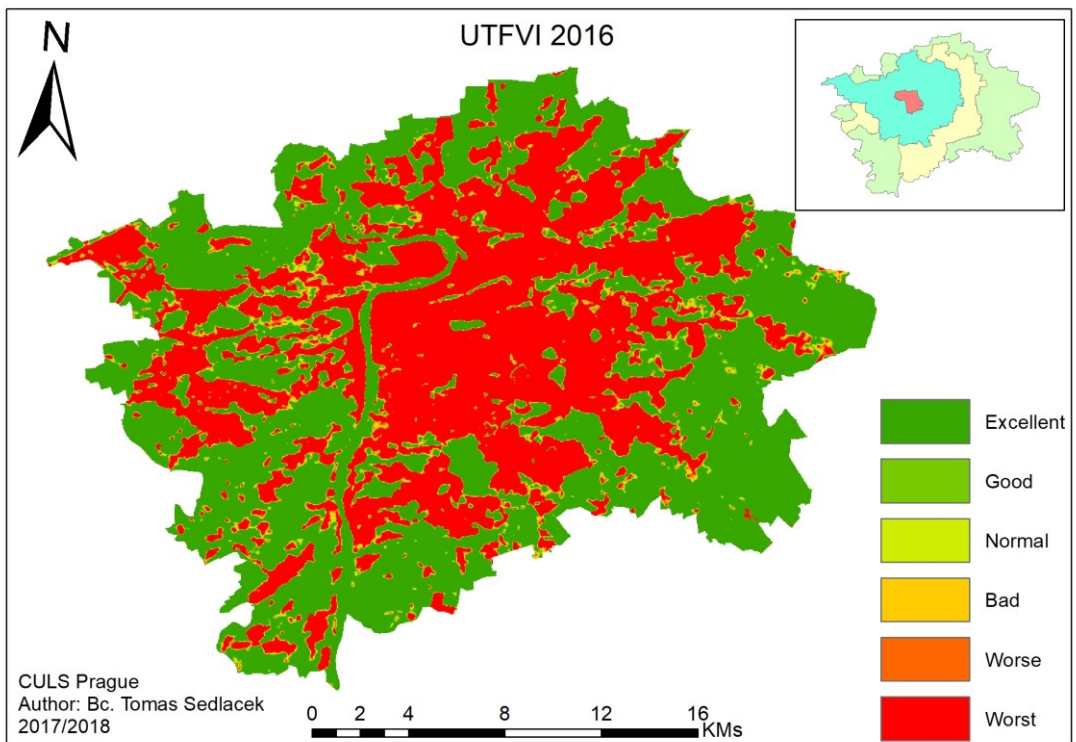
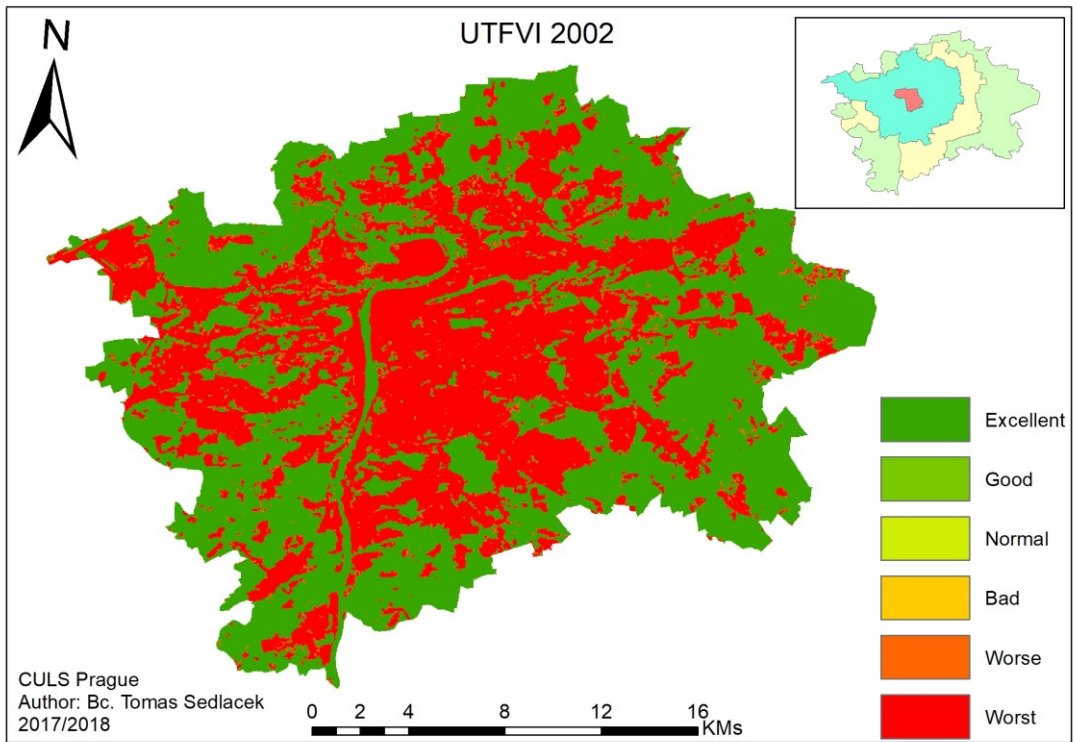
Appendix 3: Concentric zones of Prague (Author).



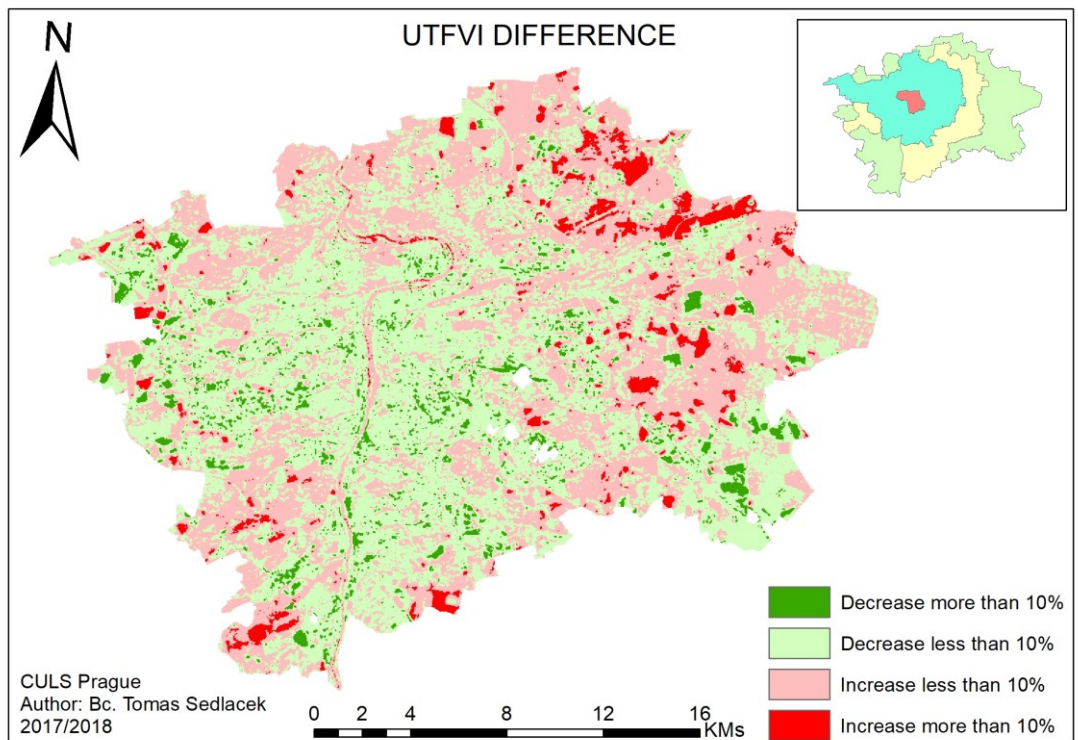
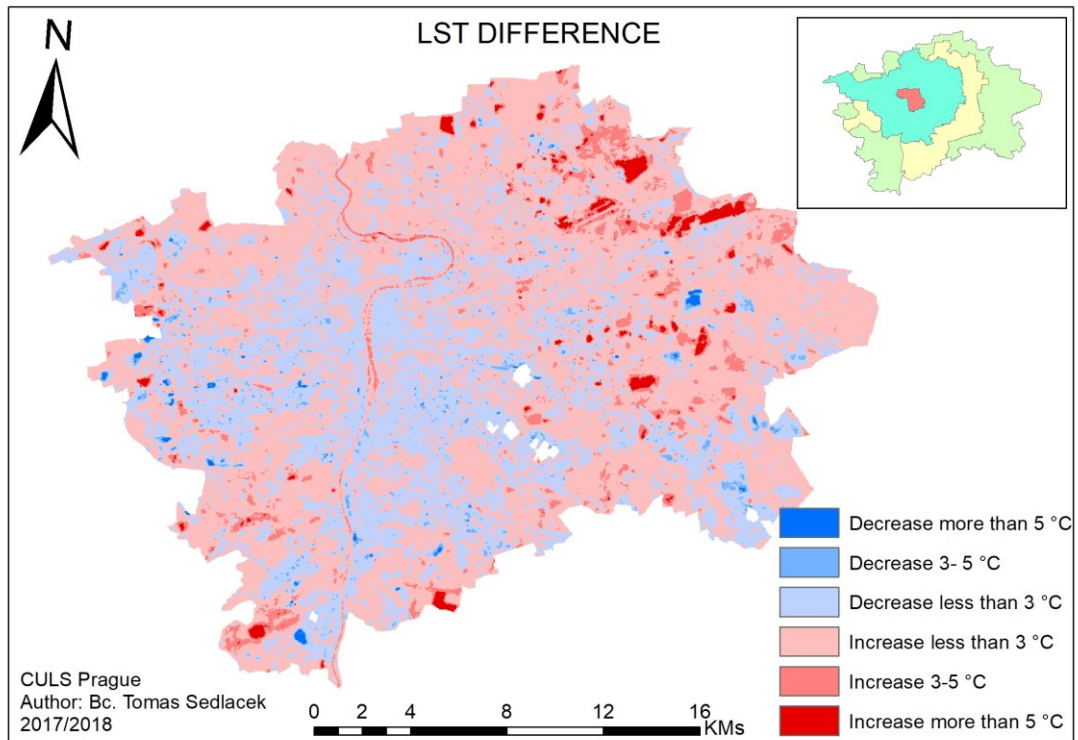
Appendix 4: NDVI and BI differences between 2002 and 2016 (Author).



Appendix 5: LST 2002, 2016 (Author).

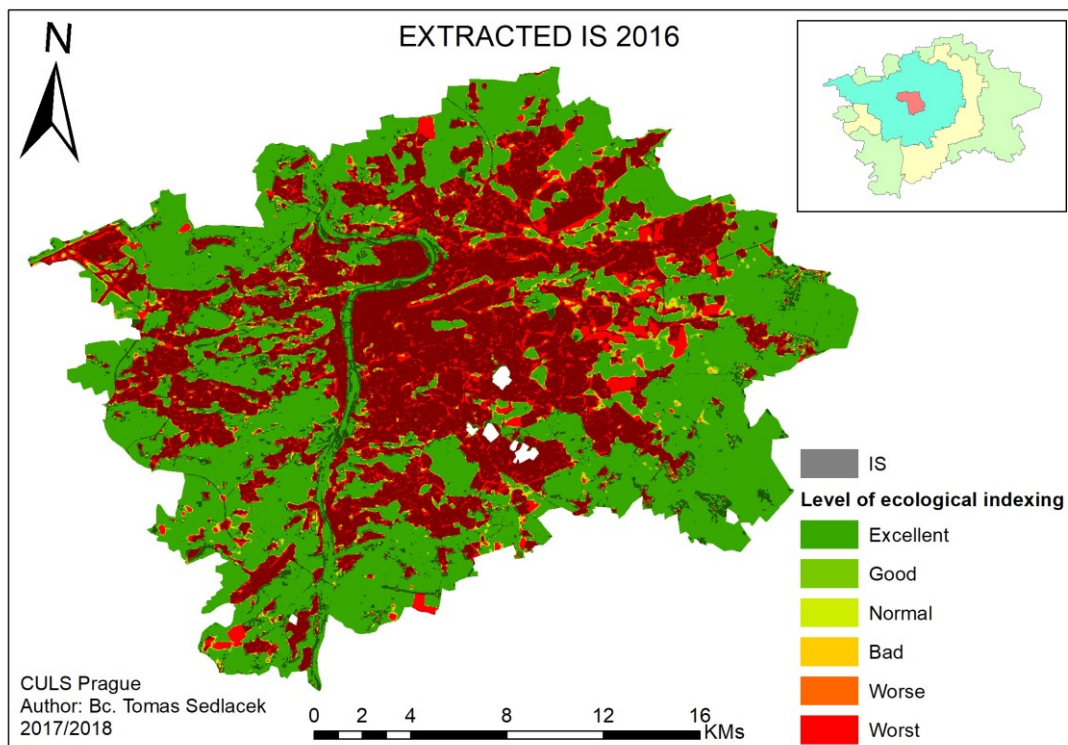


Appendix 6: UTFVI 2002, 2016 (Author).



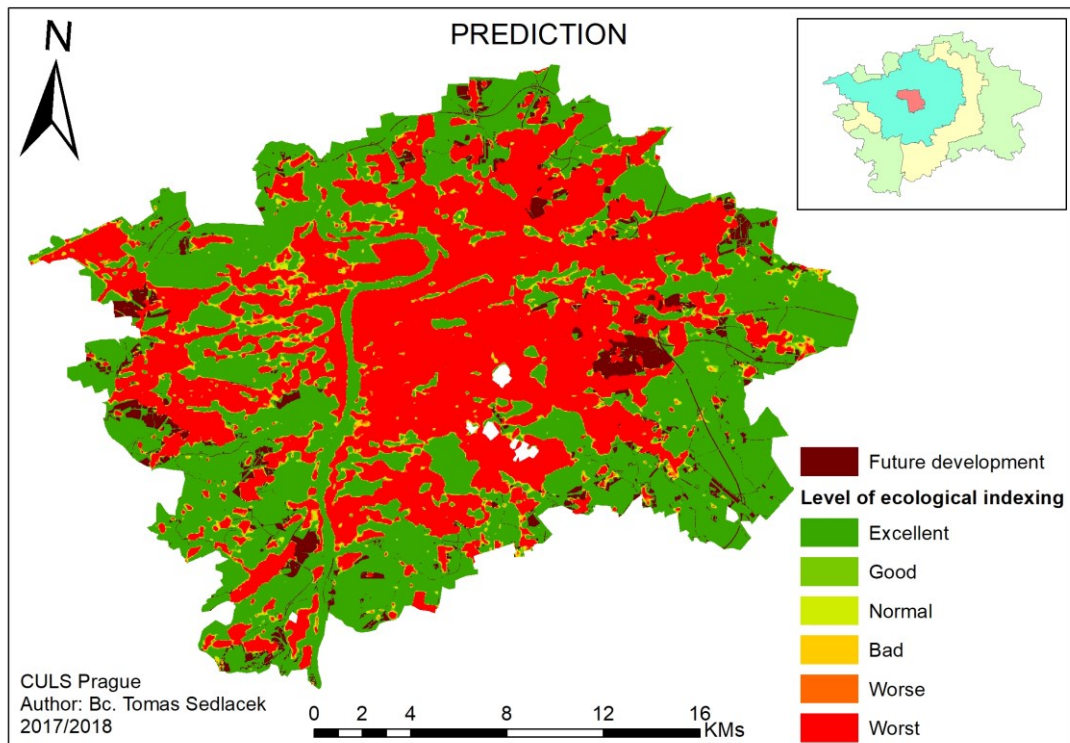
Appendix 7: LST and UTFVI differences (Author).

Mutual relation of IS and UTFVI 2016						
Level of UTFVI	1	2	3	4	5	6
Area of IS (hectars)	2 172	358	453	527	566	16 849
Share	10,38%	1,71%	2,16%	2,52%	2,71%	80,52%



Appendix 8: Relation of IS and UTFVI 2016 (Author).

Increase of UTFVI (Worst level)	
Downtown	0,00%
Inner city	3,00%
Outer city	9,70%
Outskirt	35,50%
Prague area	11,89%



Appendix 9: Prediction of near future development (Author).